Spring 5-1-2014

Effect of Particle Shape and Size on Compressibility Behavior of Dredged Sediment in a Geotextile Tube Dewatering Application

Louis Lafata

Effect of Particle Shape and Size on Compressibility Behavior of Dredged Sediment in a Geotextile Tube Dewatering Application

A Capstone Project Submitted in Partial Fulfillment of the
Requirements of the Renée Crown University Honors Program at
Syracuse University

Louis Lafata
Candidate for BS Civil Engineering Degree
and Renée Crown University Honors
May 2014

Honors Capstone Project in Civil Engineering

Capstone Project Advisor: _____
Shobha K. Bhatia, Laura J. and L. Douglas Meredith Professor

Capstone Project Reader: _____
Mahmoud Khachan

Honors Director: _____
Stephen Kuusisto, Director

Date: April 23rd, 2014

Abstract

Each year, more than 250 million cubic yards of sediment need to be dredged from U.S. ports, harbors and waterways to maintain navigability. This is accomplished by dredging, the process of excavating submerged sediment by means of scooping or suction. Dredged sediments have low solids content, typically between 10% and 20% for hydraulic dredging. Geotextile tubes are one of many methods utilized to dewater these sediments, which is a process of removing water from sediment that contains low percent solids. Understanding the engineering behavior of slurries inside geotextile tubes is critical for the evaluation of the properties of the dewatered sediments. This study explores the effect of particle shape and size of fine sediments such as silt, subrounded sand and spherical glass beads to assess their particle network compressibility and compressive strength behaviors, which will enable the determination of the ultimate solids content that these sediments can obtain in a geotextile tube environment. Sediments that are more spherical have shown to achieve higher initial and final solids contents. Sediments that are more spherical also achieve their maximum packing structure at lower compressive forces compared to sediments that are less spherical. Less spherical sediments have shown to rearrange gradually with each successive compressive force to achieve the optimal packing structure, representative of the continuous reorientation of the particle network.

Table of Contents

Executive Summary

The magnitude of dredging operations required in the United States each year to maintain the nation's ports, harbors and channels is immense. More than 250 million cubic yards of sediments need to be dredged annually. Dredging is the process of excavating submerged sediment by means of scooping or suction for purposes such as land reclamation, contaminant remediation and seabed mining. During dredging processes that are hydraulic, sediments are converted to a slurry form. Slurry is a mixture of suspended soil particles and water that contains a low percentage of solid material. In order to efficiently manage these slurries, dewatering processes must be implemented. Dewatering is the removal of water from the slurry, effectively increasing the percentage of solids. Geotextile tubes are one of many methods utilized to dewater these sediments. Slurry is pumped into a geotextile enclosure, which allows water to permeate out of the tube while sediments are retained. Geotextile tube dewatering is an inexpensive way to dewater slurries and the tubes have many beneficial end uses including shoreline protection, beach enhancement and jetty construction.

Understanding the engineering behavior of slurries inside geotextile tubes is critical for the evaluation of the properties of the dewatered sediments. The dewatering time and final solid contents are needed to evaluate the feasibility of the project. Significant research exists that evaluates the overall performance and modeling behavior of geotextile tubes. Several investigations have evaluated the filtration efficiency as well as percent dewatered of the slurries. Other researchers have explored the strict geotechnical behavior of sediments such as particle size distribution and particle shape. The bridging of these two research areas in the context of a geotextile tube dewatering application has not been investigated. This research will examine the

behavior of sediments that vary in particle size and shape to delineate the influence of their properties in the context of geotextile tube dewatering.

In a geotextile tube, several processes take place simultaneously as slurry is pumped into the enclosure. As slurry is pumped, sedimentation begins and particles begin to settle to the bottom of the tube. Naturally, the largest particles will settle first while the finer particles remain suspended for a longer period of time. This sedimentation process continues and soon produces a layer of sediment at the bottom of the tube, called a filter cake. This layer of sediment ultimately compresses due to the weight of the water, sediment and pumping pressure above it. This compression is largely a function of sediment properties such as particle size distribution and the nature of sediment particles. Exploring the effects of sediment properties on the filter cake behavior is an important part of understanding how geotextile tubes perform in the field.

To assess the compressibility of filter cake sediment in relation to particle shape and size distribution, centrifuge compression tests were performed. The centrifuge applies different amounts of force to a slurry and the change in height of the sample is measured. The height of the sample is directly related to the percentage of solids contained, which is the ultimate parameter being measured. For this study, three different types of sediments were tested including glass beads, Ottawa Sand and Tully Silt, each having differing particle size distributions and shapes. Glass beads are nearly perfect spheres, Ottawa sand is subrounded and Tully Silt is an angular material. Each type of sediment was tested using the three different size ranges of 105μm-177μm, 177μm-250μm, and 250μm-297μm.

Noticeable differences in results were found with varying particle size and shape of the materials tested. Spherical glass beads showed quick changes in sample height while the less spherical Tully Silt showed a gradual compression. Sediments of smaller particle sizes have structures that are more compressible because there is a larger amount of void space between

particles. When the number of sediment particles is increased, the amount of void space in the particle network increases allowing for larger amounts of particle network compression. More spherical sediment particles show a higher initial percent solids immediately after naturally settling as well as higher final percent solids after compression, indicative of the natural packing ability of the sediment. More spherical sediment reaches maximum packing density at a lower force while less spherical material requires a greater force for the same effect. Given these findings, practicing engineers and researchers can better determine the final solids content of a slurry based on its particle size distribution and particle shape. In addition, the total amount of slurry that can be pumped into the tube can be estimated.

Acknowledgements

I would like to express my sincere gratitude to my research advisor Dr. Shobha Bhatia, who has supported my professional development throughout my research experience. Dr. Bhatia's patience and knowledge is exemplary and she has been an excellent mentor. Dr. Bhatia initially offered me a research position during the summer of 2013, and I have had an exceptional experience working under her supervision ever since. She has provided me an immense amount of knowledge and has always been helpful in answering questions and guiding my work.

I would also like to thank my lab coworkers Mahmoud Khachan and George Segré. Mahmoud has always offered encouraging and constructive feedback on my work and has been extremely supportive and motivating. During the times I have worked with George, he has been dependable and encouraging.

In addition, I would like to thank the L.C. Smith Department of Civil and Environmental engineering and the National Science Foundation (CMMI 1100131) for providing the technical, professional and financial resources that have contributed to my successful experience.

1. Introduction

It is estimated that in the United States alone, approximately 250 million cubic yards of dredged sediment needs to be removed annually in order to maintain the navigability of the nation's ports and harbors (U.S. Army Corps of Engineers, 2013). Sources of dredged material range from coarse non-cohesive beach sand to relatively fine cohesive material with organics (Figure 1). Dredging is necessary in various circumstances, primarily due to the ongoing process of sedimentation. Sand and silt grains, with particle sizes ranging from 0.002mm-2mm flow downstream in rivers eventually settling and filling channels, reducing navigability (U.S. EPA, 2012). The majority of dredging operations are performed in order to deepen channels and berthing areas for ship passage. Operations may also be executed to prevent the spread of contaminants in a water body or to prevent human or biota exposure.

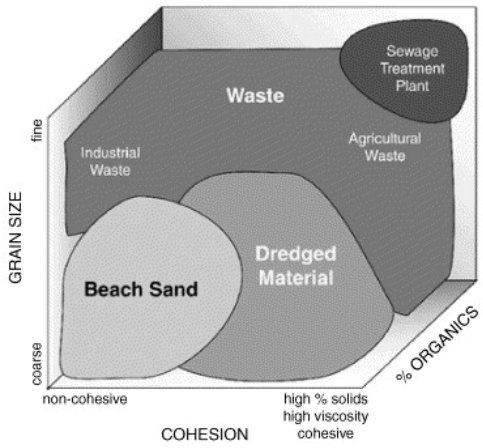

Figure 1: *Illustration of Engineering Properties of Dewatered Sediments in Geotextile Tubes (Gaffney, 2001)*

Dewatering is a process by which the solids content of sediment is increased using mechanical technologies such as centrifuges or belt filter presses as well as non-mechanical processes such as

lagoons and sand drying beds. Dewatering is used in various industries that handle sediments that range from noncohesive coarse beach sand to ultra-fine organic agricultural and sewage treatment plant waste. These sediments and wastes can possess different amounts of organic material, have various grain sizes and vary in cohesiveness. However, the dredging industry primarily deals with high percent solids material that has moderate to high levels of cohesion, coarse to fine grain sizes and low to moderate organic content. Dredging can be performed either hydraulically or mechanically. Hydraulically dredged sediments typically have a solids content of 10-20%, whereas mechanically dredged sediments have a solids content close to 50% (U.S. EPA, 2012). Geotextile tube dewatering is a process that will allow the safe and efficient disposal of sediment that has a low percent solids content. The process also offers the advantage of minimal environmental impacts, ease of construction and beneficial end-use applications (Fowler, 1996).

A geotextile tube is a fabric enclosure that is formed by sewing permeable but soil-tight geotextiles together for the purpose of allowing water to permeate through the tube while retaining solid material (Moo-Young, 2002). Woven geotextiles are commonly used, made of polypropylene or polyester material. For geotextile tube dewatering, the primary concern is being able to predict the ultimate solids content that can be obtained inside the tube as well as the rate at which dewatering will occur. Understanding the behavior of the sediments that are pumped into a geotextile enclosure is important for predicting the behavior of the sediment, particularly the settling behavior and rate of compression and/or evaluating the performance of the tubes. Knowing the behavior of sediment will allow for more accurate design prediction of the ultimate solid content in the geotextile tube and total dewatering time.

2. Scope of Study

In order to optimize the efficiency of geotextile tube dewatering processes, it is important to understand the behavior of the specific sediment that will be pumped into the enclosure. In this study, fine sediments such as silt, subrounded sand and spherical glass beads are investigated to assess their particle network compressibility and compressive strength behaviors, which will enable the determination of the ultimate solids content that these sediments can obtain in a geotextile tube environment.

3. Literature Review

3.1 *Geotextile Tube Performance Tests*

Researchers and practicing engineers have used several types of tests to assess the overall performance of geotextile tubes and the evaluation of performance parameters such as dewatering rate and filtration efficiency (Grzelak et al., 2011). Bench scale tests such as the falling head test, pressure filtration test and geotextile tube dewatering test are used for the measurement of the overall tube performance and suggest a standard for industry (Grzelak, 2011).

In recent years, researchers have made significant progress with understanding the sediment characteristics that control dewatering behavior. For example, it has been demonstrated that slurry characteristics such as the concentration of solids govern the dewatering rate of sediments (Satyamurthy, 2008). Huang and Luo (2007) show that geotextile tube filter cake heights are linearly correlated to the sediment void ratio, compressibility, particle size distribution, plasticity index and organics and mineral composition. For this study, falling head dewatering tests were

performed with four different types of woven geotextiles. It was found that the dewatering efficiency and the system's final permittivity were governed by the thickness and void ratio of the filter cake rather than the permittivities of the geotextiles used.

3.2 *Sediment Properties*

Significant research also exists that explores the effect of particle shape on various geotechnical engineering properties, notably packing density, stiffness and strength. Santamarina & Cho (2004) have noted that angularity and roughness create decreases in small strain stiffness and residual friction angle. Cubrinovski (2002) has considered the effects of particle shape on the minimum, maximum and change in void ratio for cohesionless soils, and Witt & Braun (1983) have demonstrated the effect of particle flatness, orientation and stratification on soil permeability.

Particle shape also has an effect on the compressibility behavior of sediment, which directly correlates to the compressive yield stress. Cho and Dodds (2006) have shown that a decrease in the sphericity/roundness of a particle results in an increase in compressibility under a zero-lateral strain loading. This suggests that an increase in particle irregularity results in increased reorientation of particles when subjected to a compressive force. When a given sediment slurry is compressed, the applied stress induces a decrease in the slurry height, which correlates to an increase in the percentage of solids. For Cho and Dodds' study, particle sizes that were tested ranged from 0.9mm to 1.3 mm with most sizes in the range of 0.15mm to 0.6mm. Nasser and James (2006) describe the compressive yield stress as the stress that must be exceeded by an applied stress before consolidation will occur and the percent solids will increase. An increase in compressive stress will continue to result in a decrease in sample height and an increase in

percentage solids until an ultimate value has been attained and no further compression occurs. De Kretser et al (1997) describe this interaction process as the network strength at all depths in the sediment being in equilibrium with the compressive force at all depths.

The compressive behaviors of sediments have important implications for geotextile tube dewatering applications. The compressibility behaviors of sediment as well as other sediment characteristics such as the grain size distribution, percentage of organics and plasticity are important parameters to understand for design applications. The ultimate percentage of solids and final volume of sediment that can be pumped into the geotextile tube can be predicted when these parameters are well understood.

3.3 *Centrifuge Compressibility Tests*

Researchers have conducted centrifuge compression tests in many applications on a range of sediments and materials with varying particle sizes. The chemical process industry typically conducts tests on particulate suspensions to measure behaviors such as settling, separation and compressibility where particles are generally in the range of 0.1μm-2μm in diameter. The mining industry also utilizes centrifuge tests for separation and dewatering industrial wastes. For mining applications, particle size ranges are similar to the chemical industry but can reach sizes up to 10μm in diameter. Centrifuge compression tests involve the measurement of the sediment interface height of sediment and material of certain solids content at increasing values of stress. Based on these results, the compressive yield stress and the solids content of a material is determined. One widely used method to determine these parameters is the mean value approximation, proposed by Buscall and White (1987). Nasser and James (2006) calculated volume fraction □ compressive yield stress P_y(□) and of bentonite suspensions using this

technique. In this study, the diameter of the kaolinite particles tested ranged between 0.1µm to 2µm. De Kretser et al (1997) utilized this technique to examine the compressibility of clay tailings with particle sizes ranging between 1µm and 10µm in diameter. This study determined that a power law correlates the percent solids of the clay tailing solids to the compressive strength of the material (Figure 2). Figure 2 shows the increases in compressive yield stress relative to the increase on slurry percent solids. As higher compressive forces are applied to the slurry, the particle network compresses, obtaining a higher percent solids. Channell and Zukoski (1997) have also used this method for aggregated alumina suspensions of an average particle diameter of 1.3µm. Curvers et al. (2009) have used centrifugation for the assessment of wastewater treatment sludge suspension compressibility at low pressures between 0.27-0.34 Pascal.

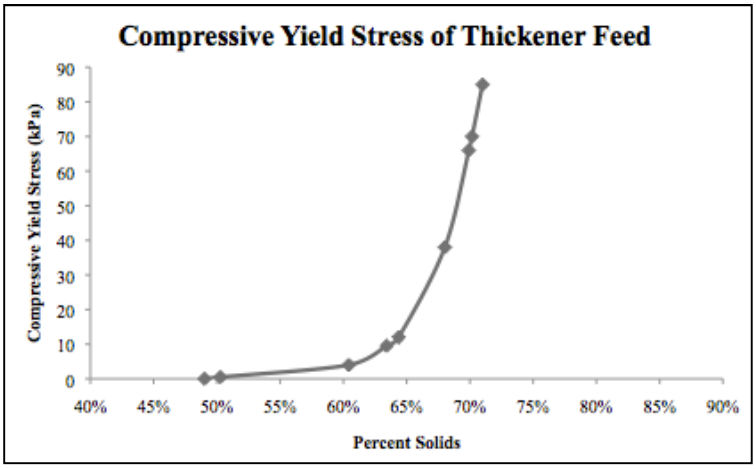

Figure 2: *Re-plotted Relationship between Percent Solids and Compressive Yield Stress (De Kretser et al., 1997)*

Miller et al. (1996) analyzed the compressive rheological responses of flocculated kaolin and alumina suspensions of particle sizes of 0.2µm to 0.5µm using pressure filtration and centrifugal compression. The volume fraction profile as well as the sediment height were examined at

various speeds. It was noted that the compressive yield stress of each suspension increases rapidly with volume fraction and increases with the inverse square of particle size. Miller et al. have also concluded that although increased mechanical loads do not always result in an increase in volume fraction, the similar increases in volume fraction are controlled by the force needed to rearrange the particle network.

Given this wealth of knowledge, there is no such study that attempts to isolate particle size and shape effects on sediment compressibility specifically within the scope of a geotextile tube dewatering application. The studies that have been done have focused on either performance based tests, macroscale behavior of sands or compressibility behavior of fine particles in chemical applications. Current study will incorporate the centrifuge compression testing procedures and developed formulas like the Mean Value Approximation (Buscall & White, 1987) to examine the behaviors of coarser sediments in a geotextile tube application. Studying the effect of particle shape and particle size of sediments typically used in geotextile dewatering using centrifuge compression testing will give a more thorough understanding of the compression behavior of the sediment in dewatering applications. The overall goal of this study is to bridge the gap in research between macroscale behavior of sediments and their compressibility behavior in the geotextile tube dewatering application.

4. Testing Procedures

For the selected sediments in this study, sphericity, specific gravity and centrifuge compression tests were conducted.

4.1 *Sphericity*

Sediment particle shape can be measured by a parameter known as sphericity, a measure of the degree to which the shape of a particle resembles that of a sphere. Wadell (1932) originally established a method to measure particle shape parameters, specifically sphericity. Sphericity is measured by calculating the ratio of the diameter of largest circle that can be inscribed within the boundaries of the sediment particle, to the minimum diameter of a circle that can fully encompass the sediment particle. When these two values are equal, the maximum sphericity value of 1 is achieved. Particles that are more elongated or flaky will have lower sphericities.

It is also important to consider the difference between sphericity and roundness. According to Smoltczyk (2002), roundness is related to the sharpness and curvature of the edges and corners and can be considered a measure of the roughness of particles. Figure 3 depicts a comparison of sediment particles of varying roundness and sphericity. A particle can have a high sphericity, and have either a high (0.9) or low (0.1) roundness.

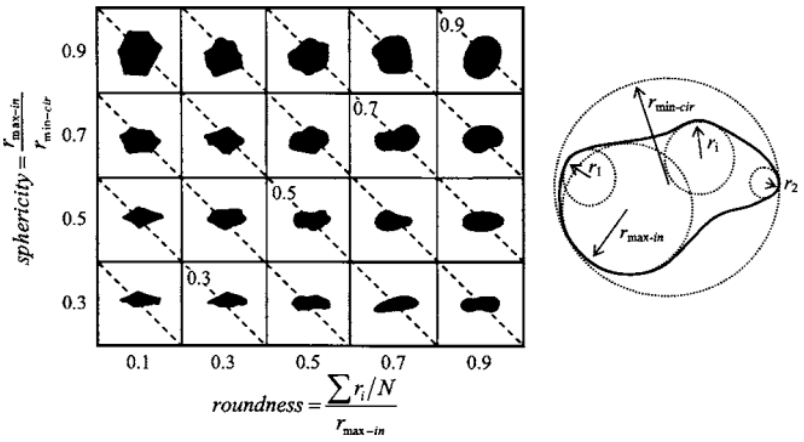

Figure 3*: Relationship between Sphericity and Roundness (Cho and Santamarina, 2006)*

In this study, sphericity is calculated using the diameter ratio suggested by Wadell (1932). Images of sediment grains were acquired using a Nikon microscope. Using ImageJ image analysis program, the sediment particle diameters were measured by their length in pixels at the given magnification. Measurements were made for approximately 50 randomly selected particles for each sediment type and size combination and average sphericity values were determined. The sphericity was calculated by dividing the diameter of largest circle (Figure 4a) that can be inscribed within the boundaries of the sediment particle by the minimum diameter of a circle that can fully encompass the sediment particle (Figure 4b). Although sphericity is a three-dimensional parameter, it is believed that using 50 sediment grains gives an accurate determination of the sphericity value because each sediment particle was placed under the microscope in a random position. Sphericity is calculated by the following formula:

$$\frac{\quad}{\quad}$$

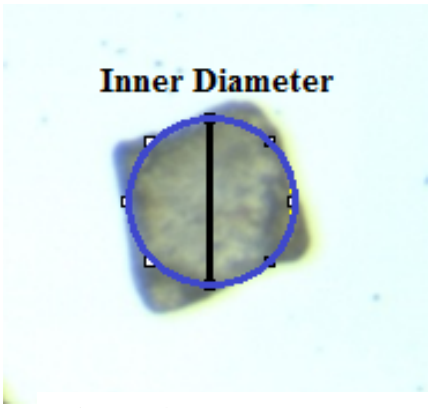

Figure 4a: *Sphericity Measurement Outer Diameter*

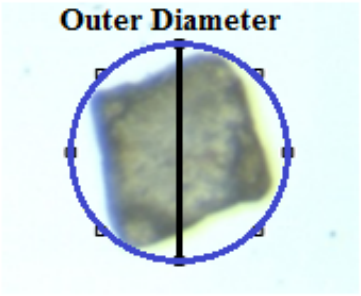

Figure 4b: *Sphericity Measurement Inner Diameter*

4.2 *Specific Gravity*

Specific gravity was determined using ASTM standard D854. Each material's specific gravity was determined using approximately 200 grams of sediment. The sediments were placed into 500mL flasks with deionized water and were allowed to remain submerged for 24 hours to ensure thorough saturation of the material. At the end of the 24 hour period, the sediment-water mixtures were placed on a Corning PC4200 hotplate and brought to a gentle boil for 10 minutes in order to remove dissolved air. Care was taken to avoid temperatures that would induce sediment loss. The flasks were the filled to the 500 mL marker with de-aired water and the mass was measured. Using this value, the mass of sediment placed in the flask, and the mass of the flask containing only de-aired water, specific gravity was calculated using the following formula:

$$Specific\ Gravity, G_S = \frac{W_0}{W_0 + (W_A - W_B)}$$

Where:

$W_0 = Weight\ of\ oven\ dry\ sediment\ sample$

$W_A = Weight\ of\ flask\ filled\ with\ water$

$W_b = Weight\ of\ flask\ filled\ with\ water\ and\ sediment$

4.3 *Grain Size Distribution*

The grain size distributions of the sediments were determined using ASTM standard D6913. Sediments were placed in a standard sieve apparatus to obtain the desired size ranges. Once the specific sediment ranges of 105µm-177µm, 177µm-250µm and 250µm-297µm were obtained, a washing sink with spray nozzle was used to wash the sediment through sieve numbers 60, 80 and

140 respectively, removing the clay fraction. This process ensures that the test results are not affected by mineralogical composition.

4.4 *Centrifuge Compression Test*

Compression tests in a Champion S-50D centrifuge (Figure 5) were performed on each sediment type for varying size ranges. Samples were prepared by placing 33.3% solids by weight into a clear tube. After adding sediment to the tubes, the remaining 66.6% of the weight of de-aired, deionized water was added. The tubes were capped, shaken vigorously for 10 seconds and quickly turned upright and placed in a holding rack (Figure 6). Once the particles have obtained their equilibrium height, this interface height was recorded. The total height of the water was also recorded for determination of the tube's overall percent solids.

Figure 5: *Champion S-50D Centrifuge*

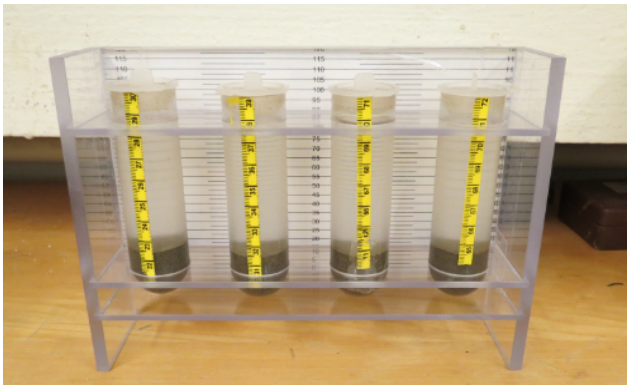

Figure 6: *Sample Test Tubes Containing Slurry*

The tubes were placed into the centrifuge and were subjected to gravities corresponding to 300, 400, 600, 800, 1000 and 1200 rotations per minute. The equilibrium sediment bed height corresponding to each gravity exerted on the sample was recorded. Buscall and White (1987) proposed a method used to determine the percent solids and the corresponding compressive yield stress using the following formulas:

$$Initial\ Volume\ Fraction\ \phi_0 = \frac{M_{soil}}{G_s * \rho_w} * \frac{1}{(\frac{M_{soil}}{G_s * \rho_w} + V_w)}$$

$$Volume\ Fraction\ \phi = \frac{\phi_0 h_0 (1 - \frac{h_{\infty+s}}{2R})}{[(h_{\infty+s})\left(1 - \frac{h_\infty}{R}\right) + \frac{h_\infty^2}{2R}]}$$

$$Compressive\ Yield\ Stress\ P_y(\phi) = \Delta\rho g \phi_0 h_0 (1 - \frac{h_\infty}{2R})$$

$$Percent\ Solids\ PS = \frac{1}{\frac{1-\phi}{\phi G_s} + 1}$$

Where:

$M_{soil} = Mass\ of\ soil\ (g)$

$G_s = Specific\ gravity$

$\rho_w = Density\ of\ water\ (\frac{g}{cm^3})$

$V_w = Volume\ water\ (cm^3)$

$h_0 = Initial\ height\ of\ slurry\ (cm)$

$s = Change\ in\ height\ divided\ by\ the\ change\ in\ natural\ log\ of\ gravity = \frac{d(h_\infty)}{d(lng)}$

$h_\infty = Height\ of\ solids\ at\ end\ of\ centrifugation\ period\ (cm)$

$R = Radius\ of\ centrifuge\ (cm)$

$\Delta\rho = Difference\ in\ density\ between\ sediment\ and\ liquid\ (\frac{g}{cm^3})$

$g = Gravitational\ acceleration\ (\frac{cm}{s^2})$

Using these equations, results in terms of □ and P_y(□) were plotted, converting from volume fraction □ to percent solids (Figure 7). Compressive strength is defined as the point at which any increase in stress will result in deformation of the sample and a resulting increase in volume

fraction. A decrease in the height of the sample results in an increase in volume fraction and an increase in the compressive strength of the sample. Each successive data point represents a specific test where a successive gravity is exerted on the sediment sample.

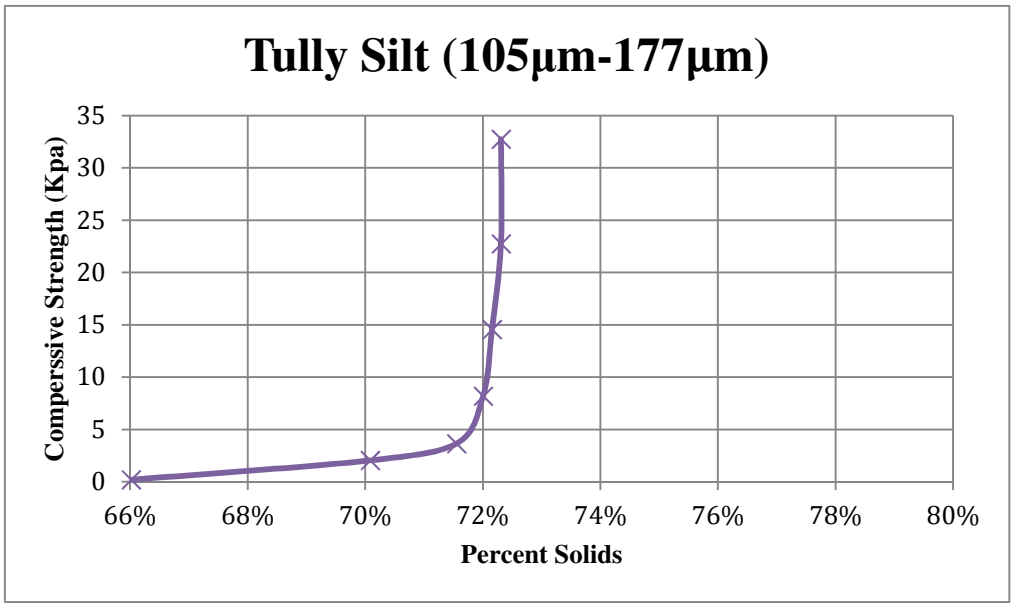

Figure 7: *Sample Test Data of Successive Gravities Exerted on Sediment*

5. Materials

Three different sediments were used in the study, including glass beads, Ottawa Sand and Tully Silt. Each of these materials has multiple size ranges and each has a different particle shape.

5.1 *Glass Beads*

Glass beads were obtained from Potters Industries, LLC in Potsdam, NY and are composed of soda-lime silica glass. Material properties for glass beads are shown in Table 1.

Table 1: Properties of Glass Beads (Given by Potters Industries)	
Unit Weight (kg/ L)	1.54
Crush Resistance (psi)	14000 - 36000
Mohs Hardness	5-6
Coefficient of Static Friction	0.9 – 1.0

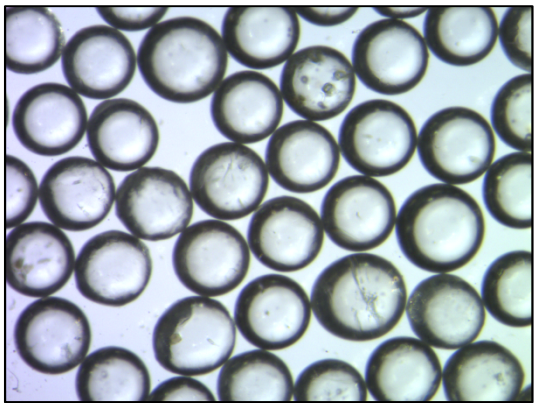

Figure 8: *Glass Beads (Scale=3.8mm)*

5.2 *Ottawa Sand*

Ottawa Sand was obtained from U.S. Silica Co. in Ottawa, Illinois, USA. Ottawa Sand is 99.8% silicon dioxide, 0.03% iron oxide, 0.06% aluminum oxide (U.S. Silica). Material properties for Ottawa Sand are shown in Table 2.

Table 2: Properties of Ottawa Sand (Given by U.S. Silica)	
D_{10} (µm)	150
D_{30} (µm)	180
D_{60} (µm)	230
C_c	1.53
C_c	0.939
Mohs Hardness	7

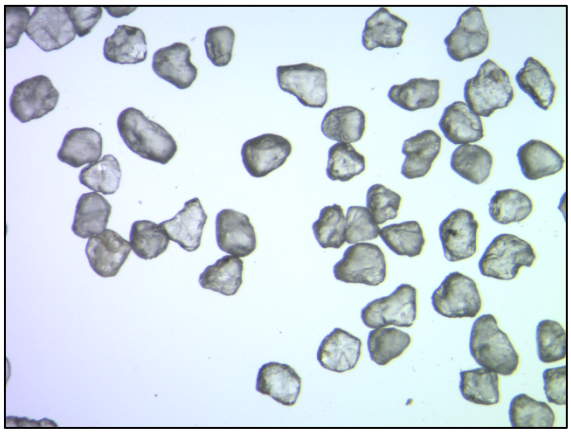

Figure 9: *Ottawa Sand (Scale=3.8mm)*

5.3 *Tully Silt*

Tully Silt was obtained from Clarks Aggregate Co. Gravel Pit in Tully, New York and was classified as silty sand (SM) per ASTM D2487. Tully Silt is composed primarily of quartz (SiO_2) and dolomite ($CaMg(CO_3)_2$). Minor components were identified as calcite ($CaCO_3$) and sylvite (KCl). Material properties for Tully Silt are given in Table 3.

Table 3: Properties of Tully Silt	
D_{10} (μm)	79
D_{30} (μm)	87
D_{60} (μm)	101
C_u	1.3
C_c	0.948
USCS Classification	SM

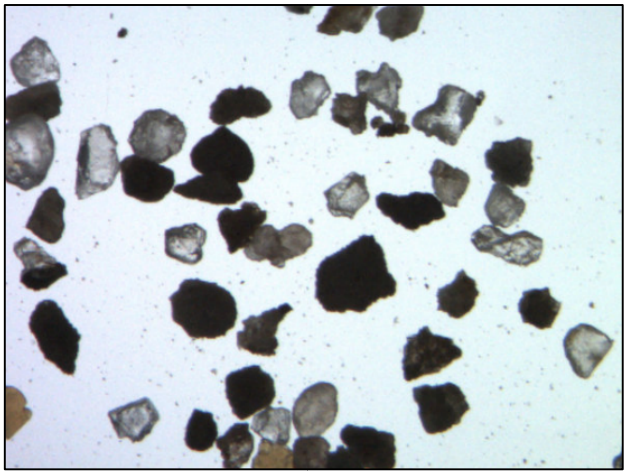

Figure 10: *Tully Silt (Scale=3.8mm)*

6. Test Results

6.1 *Sphericity and Specific Gravity*

Sphericity measurements were performed on 50 sediment particles in order to statistically represent each sample. Initially, sphericity was measured for individual sediment size ranges to ensure consistency before determining a final value for the entire sediment sample. However, this was not performed on glass beads as the product is manufactured and is not expected to show sphericity variability between differing size ranges. Images of the sediments are included in Appendix A and the sphericity calculations are included in Appendix B. The average sphericity of the glass beads ranged between 0.85 and 1.0, for Ottawa Sand it ranged between

0.52 and 0.96 and for Tully Silt it ranged between 0.386 and 0.85. The average sphericity values and ranges are given in Table 4.

Table 4: *Average Sphericity Values and Ranges of Sediment Particles*

Sediment Type	Sphericity Range	Average Sphericity	Specific Gravity, Gs
Glass Beads	0.85 – 1.0	0.988	2.47
Ottawa Sand	0.52 – 0.96	0.718	2.65
Tully Silt	0.386 - 0.85	0.630	2.66

6.2 *Compressibility Test Results*

6.2.1 Glass Beads

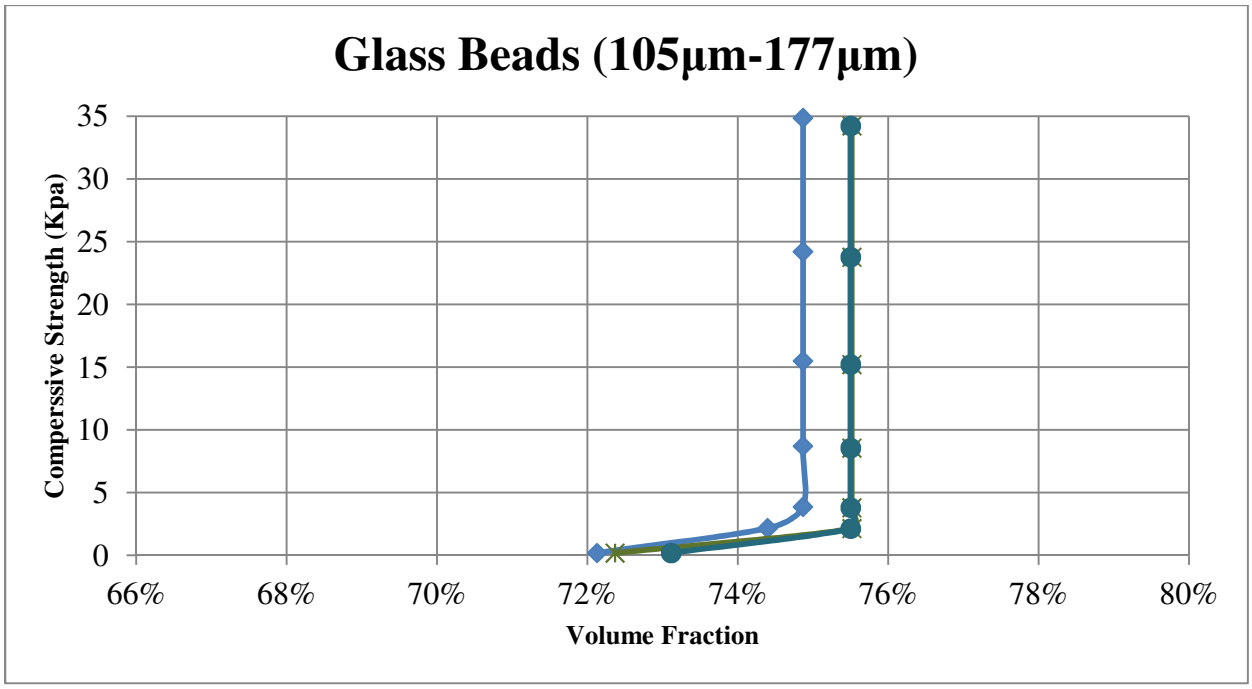

Figure 11a: *Glass Beads Size 105µm-177µm Compressibility Behavior*

Figure 11a shows test results for glass beads in the 105µm-177µm size range. The material average sphericity is 0.988. The total percent solids change is 3%. Of the three sets of tests performed, two samples achieved a final percent solids of 75% while one sample achieved a final percent solids of 75.5%.

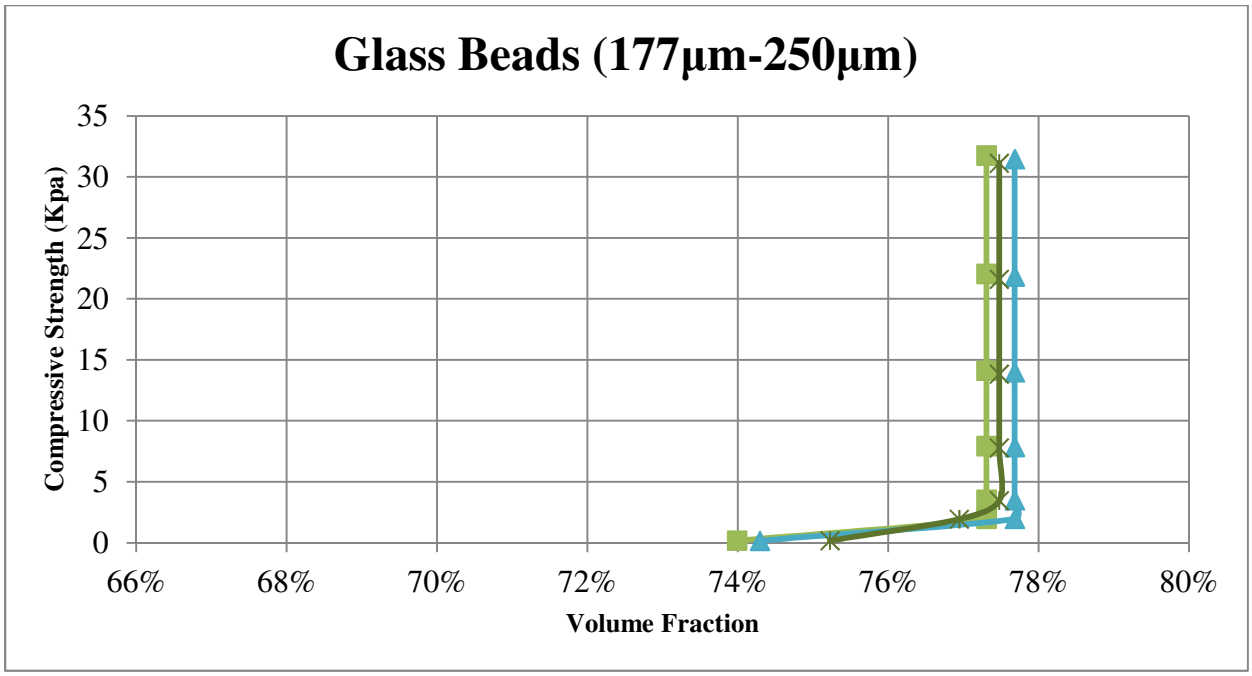

Figure 11b: *Glass Beads Size 177µm-250µm Compressibility Behavior*

Figure 11b shows test results for glass beads in the 177µm-250µm size range. The material average sphericity is 0.988. The total percent solids change is 3%. Of the three sets of tests performed, all achieved approximately 77.5% solids.

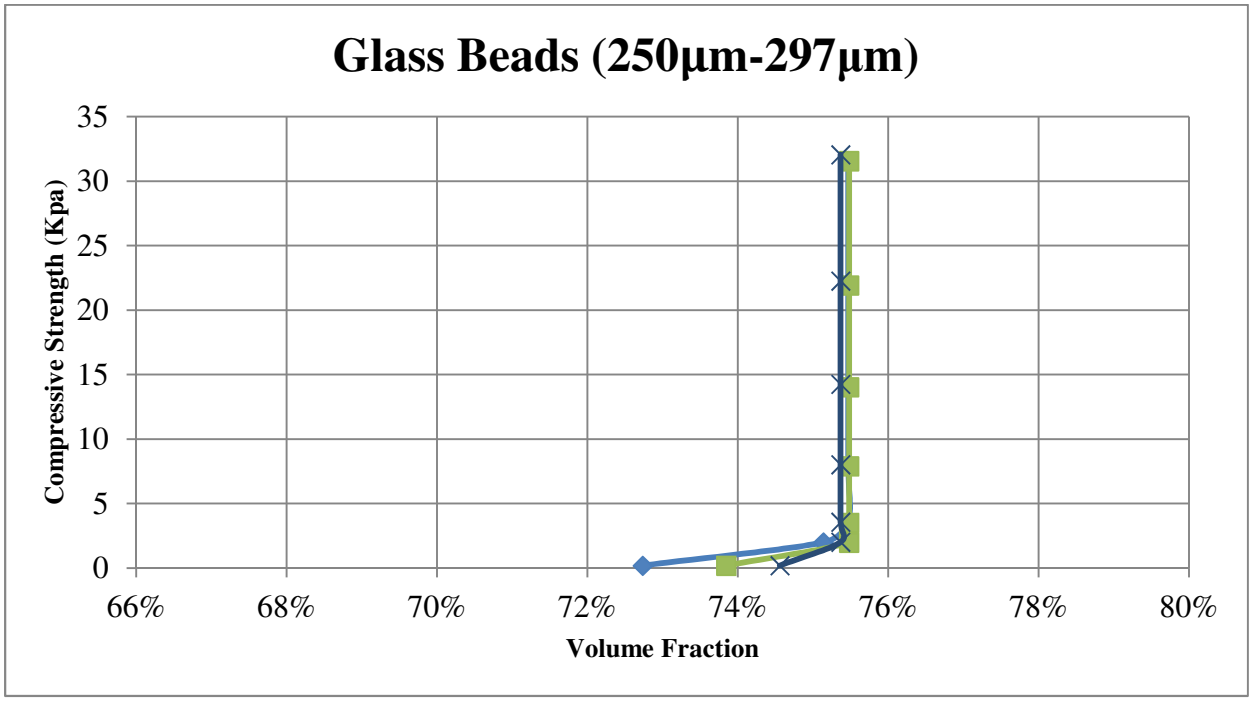

Figure 11c: *Glass Beads Size 250µm-297µm Compressibility Behavior*

Figure 11c shows test results for glass beads in the 250µm-297µm size range. The material average sphericity is 0.988. The total percent solids change is 2%. Of the three sets of tests performed, all achieved approximately 75.5% solids with little variability. This narrower sediment particle size range shows the least amount of variability of all glass bead particle sizes tested. The compressibility behavior is similar to that of the 177µm-250µm and 105µm-177µm size ranges.

6.2.2 *Ottawa Sand*

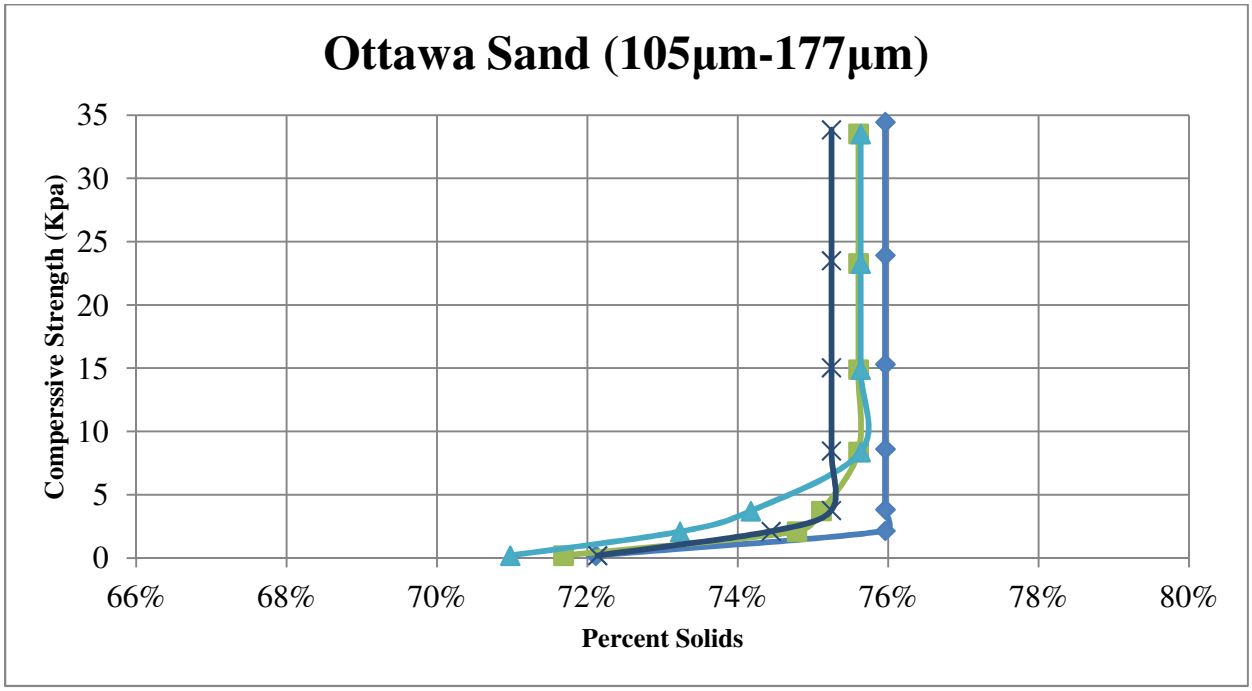

Figure 12a: *Ottawa Sand Size 105µm-177µm Compressibility Behavior*

Figure 12a shows test results for Ottawa Sand in the 105µm-177µm size range. The material average sphericity is 0.718. The total percent solids change is 6%. Of the four sets of tests performed, final percent solids ranged from 75% to 76%. The compressibility behavior is slightly different than that of the glass beads in that it is more gradual.

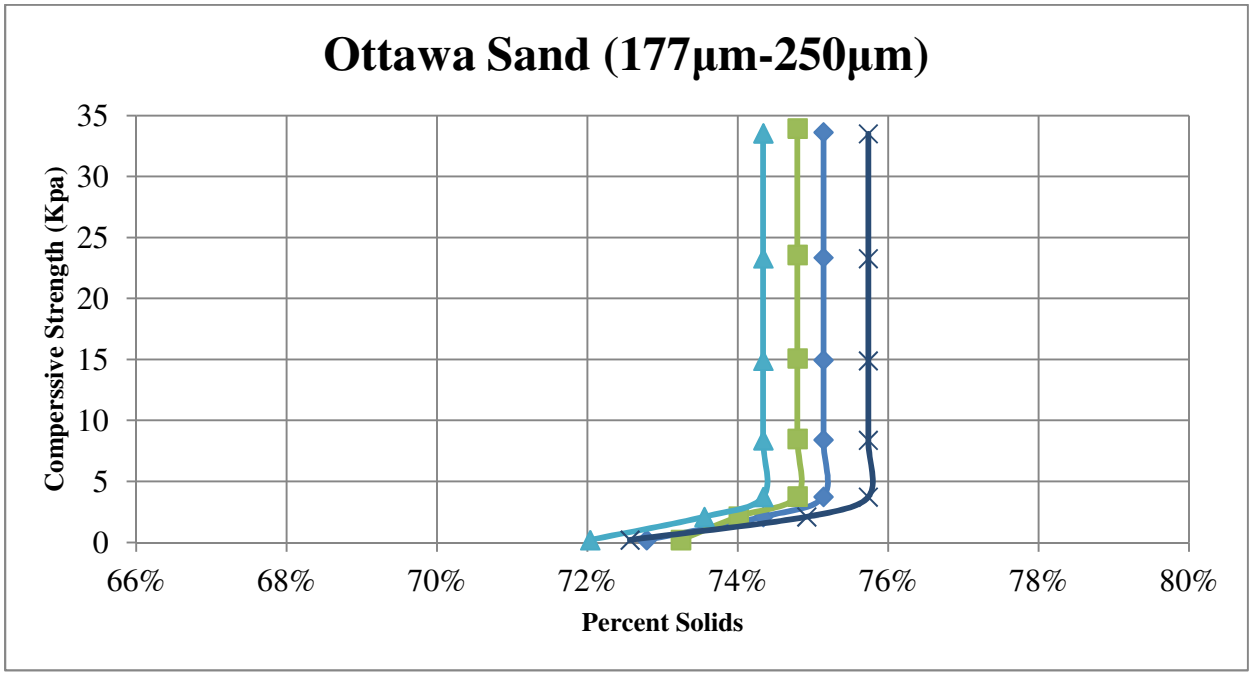

Figure 12b: *Ottawa Sand Size 177µm-250µm Compressibility Behavior*

Figure 12b shows test results for Ottawa Sand in the 177µm-250µm size range. The material average sphericity is 0.718. The total percent solids change is 4%. Of the four sets of tests performed, final percent solids ranged widely from 74.5% to 76%.

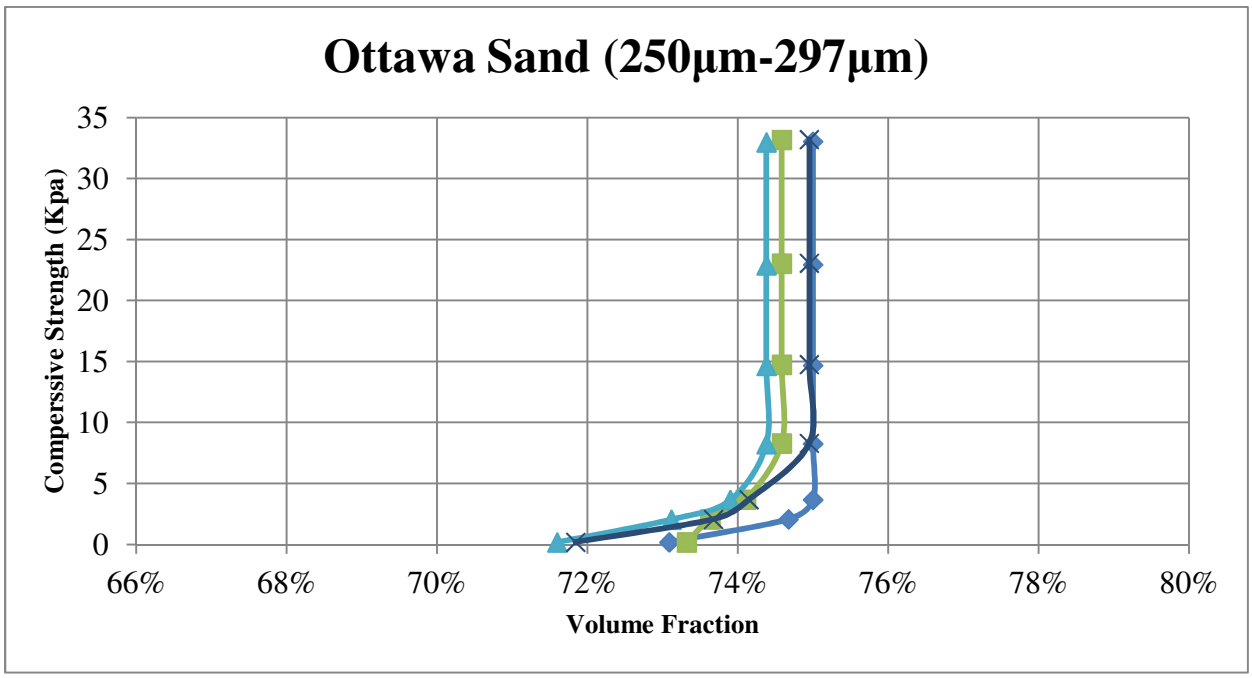

Figure 12c: *Ottawa Sand Size 250µm-297µm Compressibility Behavior*

Figure 12c shows test results for Ottawa Sand in the 250µm-297µm size range. The material average sphericity is 0.718. The total percent solids change is 2%. Of the four sets of tests performed, final percent solids ranged from 74.5% to 75%. The compressibility is similar to that of the 177µm-250µm and 105µm-177µm size ranges in that compression takes place more gradually than glass beads.

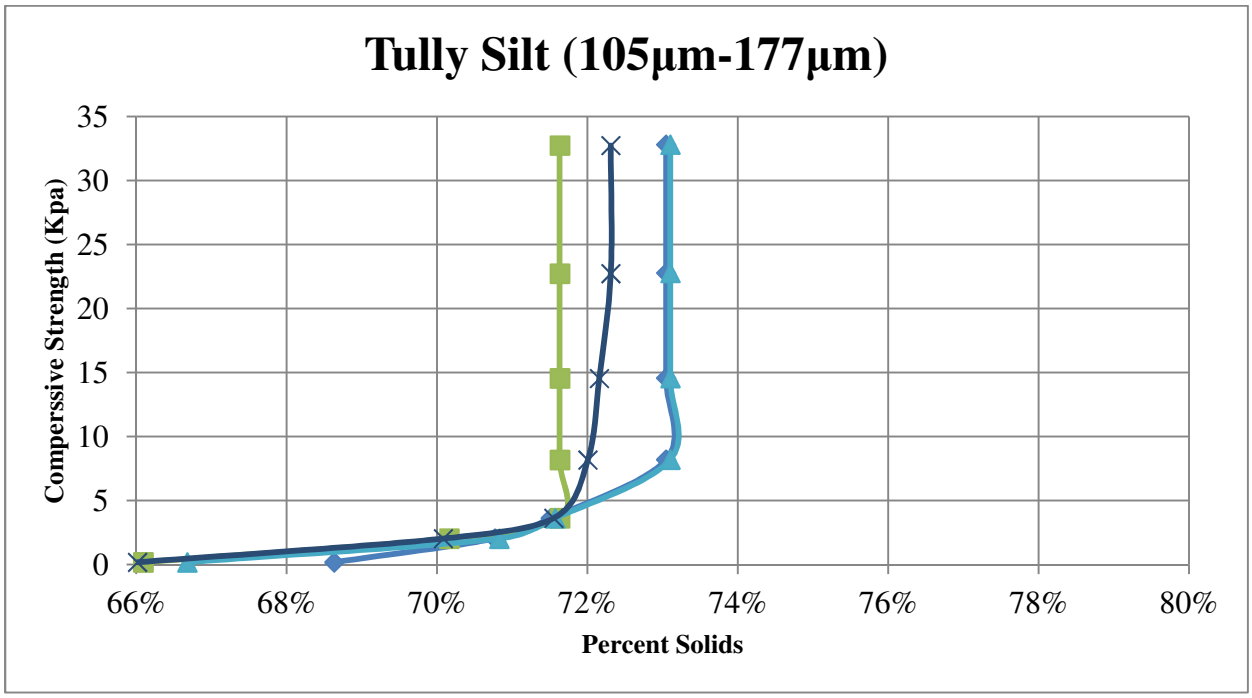

Figure 13a: *Tully Silt Size 105µm-177µm Compressibility Behavior*

Figure 13a shows test results for Tully Silt in the 105µm-177µm size range. The material average sphericity is 0.630. The total percent solids change is roughly 5%. Of the four sets of tests performed, final percent solids ranged from 71.8% to 73%. The compressibility behavior is different than that of the glass beads and Ottawa Sand in that it is much more gradual.

6.2.3 *Tully Silt*

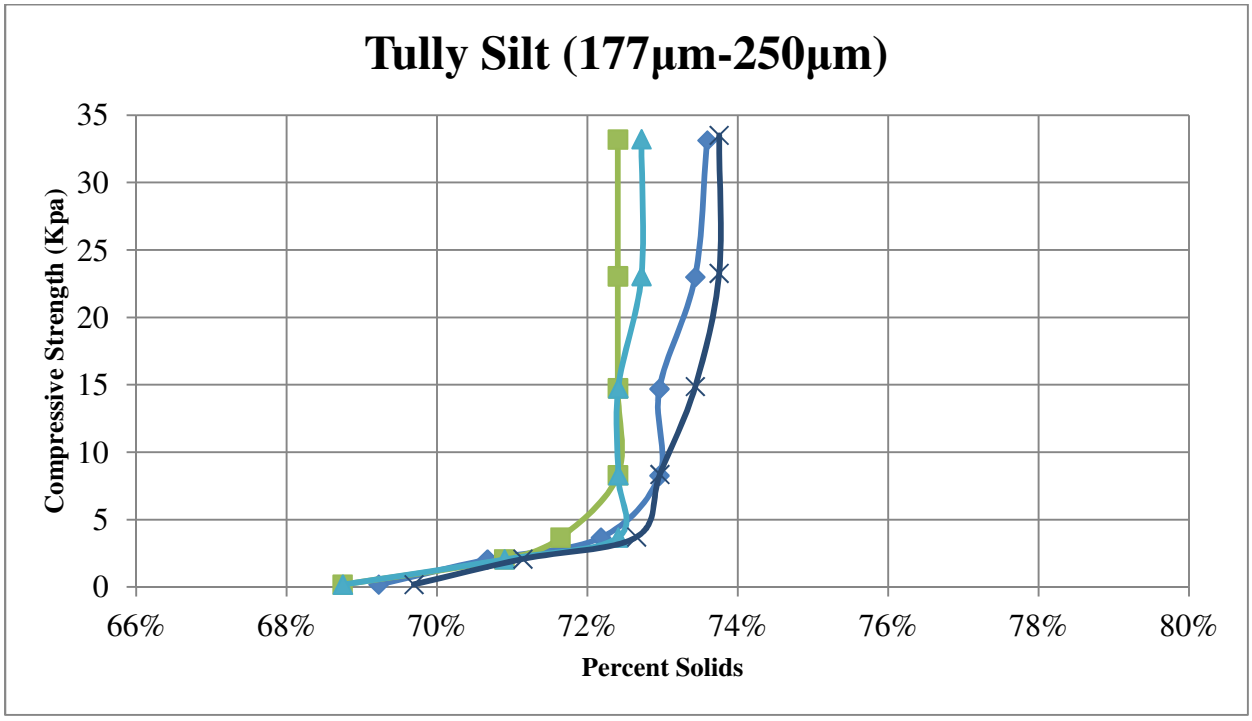

Figure 13b: *Tully Silt Size 177µm-250µm Compressibility Behavior*

Figure 13b shows test results for Tully Silt in the 177µm-250µm size range. The material average sphericity is 0.630. The total percent solids change is 3.5%. Of the four sets of tests performed, final percent solids ranged from 72.5% to 74.5%.

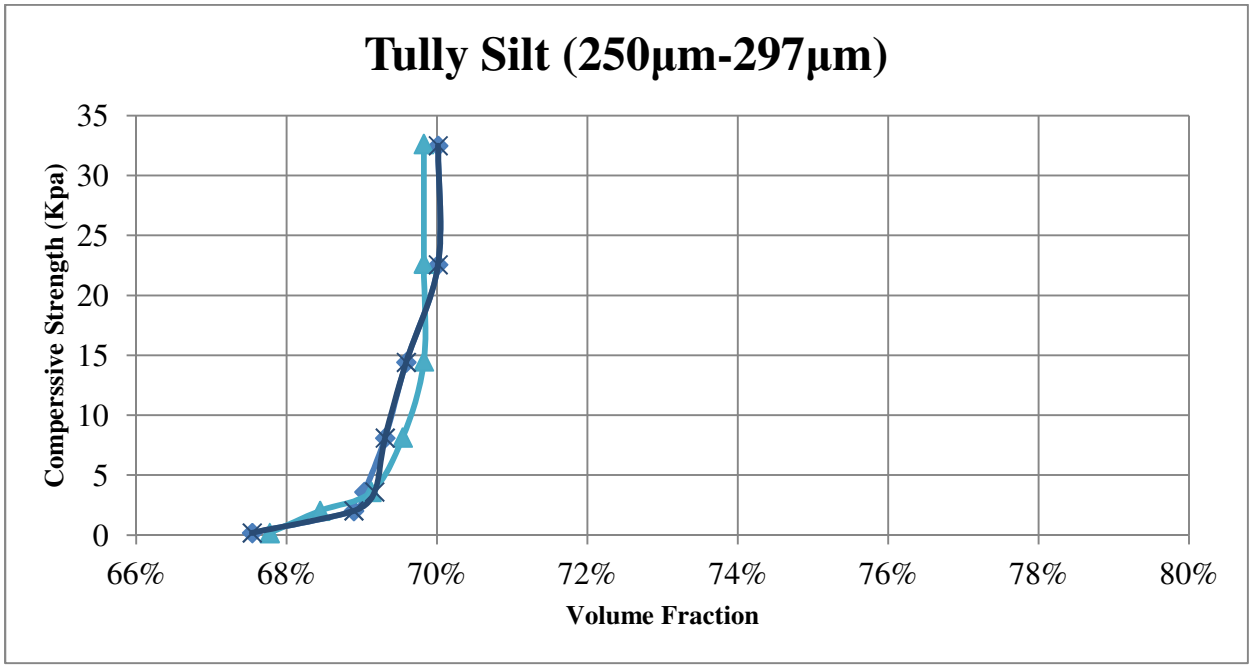

Figure 13c: *Tully Silt Size 250µm-297µm Compressibility Behavior*

Figure 13c shows test results for Tully Silt in the 250µm-297µm size range. The material average sphericity is 0.630. The total percent solids change is 2%. Of the two sets of tests performed, final percent solids attained was approximately 70%.

6.2.4 *Particle Size and Shape Comparisons*

Figures 14a, 14b and 14c show compressibility data comparisons of the varying sediment size ranges for all three sediments. These plots are average values and allow the general effect of particle size to be examined.

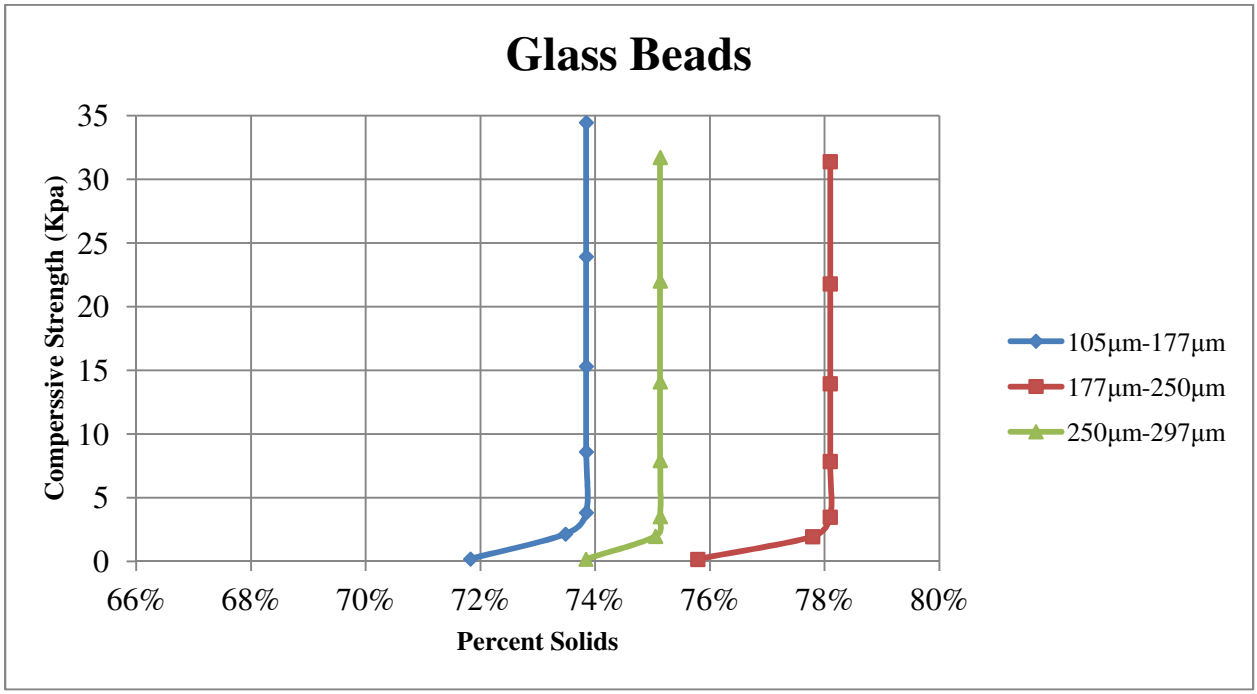

Figure 14a: *Comparison of Particle Size Range Compressibility for Glass Beads*

For glass beads, the smallest particle size range of 105µm-177µm obtained the lowest final percent solids at about 74%, whereas the middle particle size range of 177µm-250µm obtained the highest final percent solids of about 78%. The values of the largest size range of 250µm-297µm fell between the other two size ranges with a final percent solids of 75%.

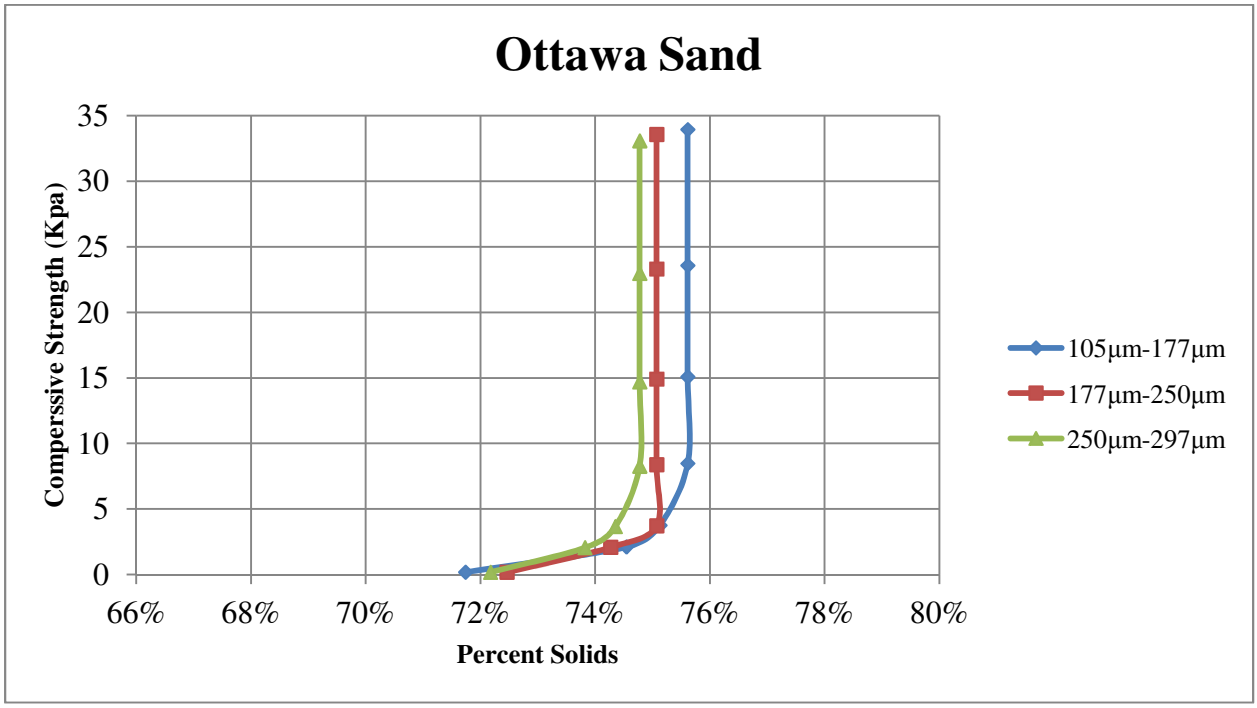

Figure 14b: *Comparison of Particle Size Range Compressibility for Ottawa Sand*

For Ottawa Sand, the smallest particle size range of 105µm-177µm obtained the highest final percent solids at about 75.8%, whereas the particles of the largest size range of 250µm-297µm obtained the lowest final percent solids of 74.8%. The middle particle size range of 177µm-250µm obtained an intermediate final percent solids value of 75%.

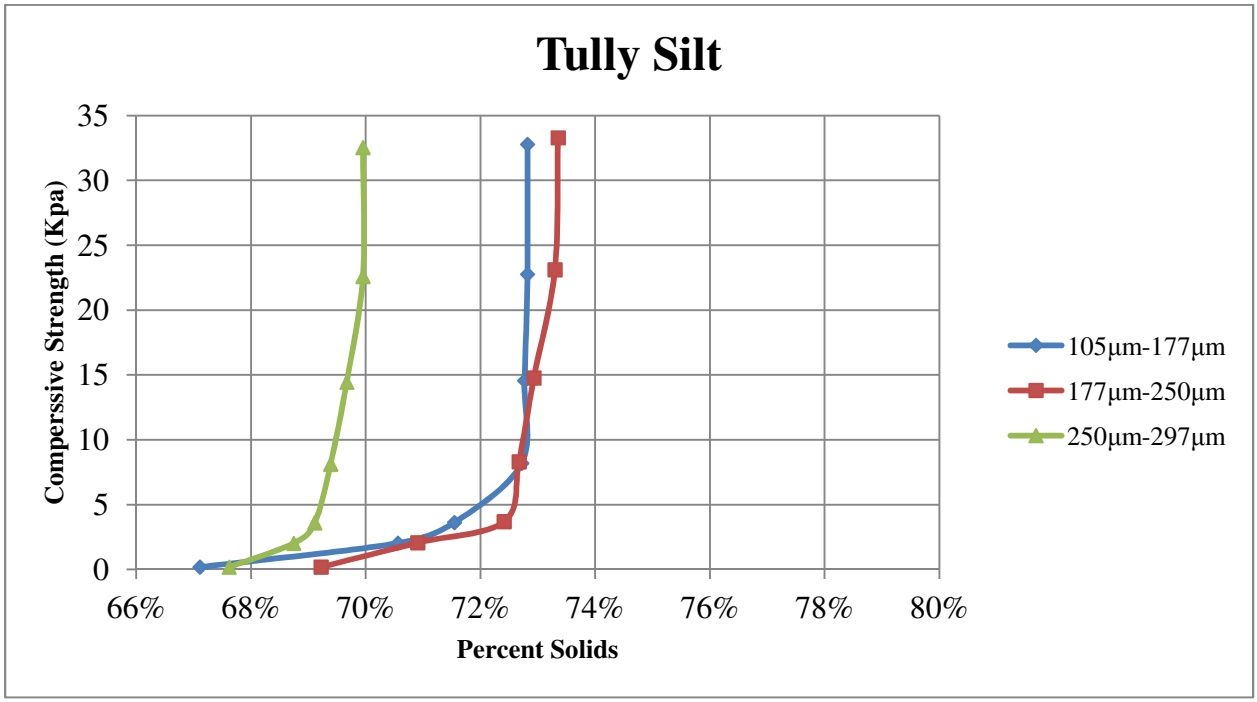

Figure 14c: *Comparison of Particle Size Range Compressibility for Tully Silt*

For Tully Silt, a relatively similar trend is seen as compared with Ottawa Sand. The particles of the largest size range of 250µm-297µm obtained the lowest final percent solids of 70%. The smallest particle size range of 105µm-177µm and the middle particle size range of 177µm-250µm obtained similar values of final percent solids, the smallest size range obtaining 72.8% and the middle size range obtaining 73.5%.

Figures 15a, 15b and 15c show compressibility data comparisons of varying sediment types for similar particle size ranges. These plots are average values and allow the general effect of particle shape to be examined.

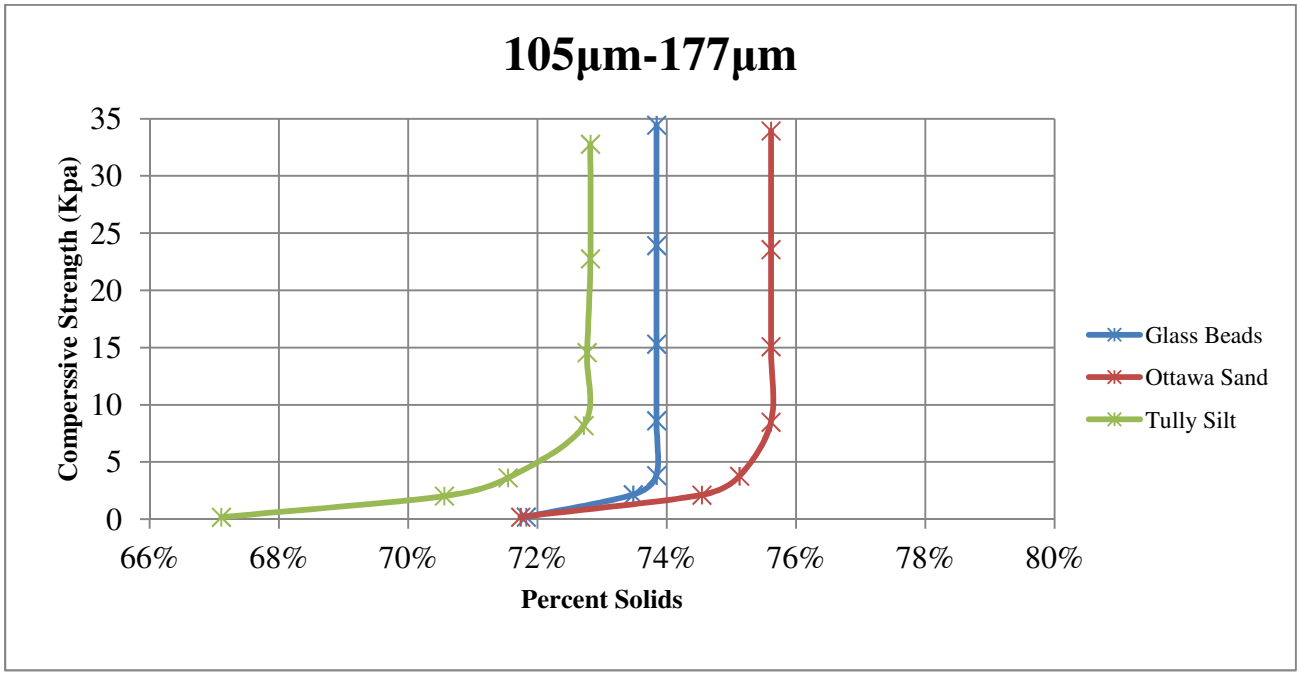

Figure 15a: *Comparison of Particle Shape Effect on Compressibility for 105µm-177µm*

For the 105µm-177µm sediment particle size range, Tully Silt (sphericity=0.63) has obtained the lowest final percent solids of approximately 73% and Ottawa sand (sphericity=0.718) has obtained the highest final percent solids of 75.8%. Glass beads (Sphericity 0.988) obtained a final percent solids in between those of the other sediment types of approximately 74%.

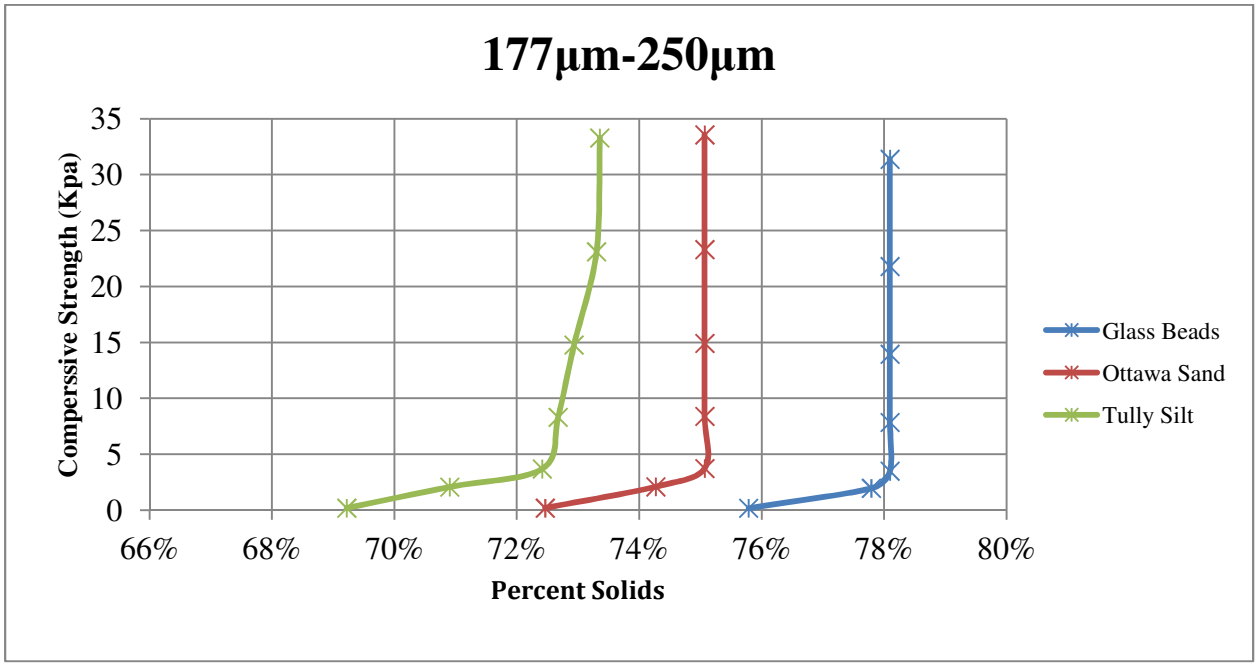

Figure 15b: *Comparison of Particle Shape Effect on Compressibility for 177µm-250µm*

For the 177µm-250µm sediment particle size range, Tully Silt (sphericity=0.63) has obtained the lowest final percent solids of approximately 73.5% and glass beads (sphericity=0.988) obtained the highest final percent solids of 78%. Ottawa Sand (sphericity=0.718) obtained a final percent solids value in between those of the other sediment types of approximately 75%.

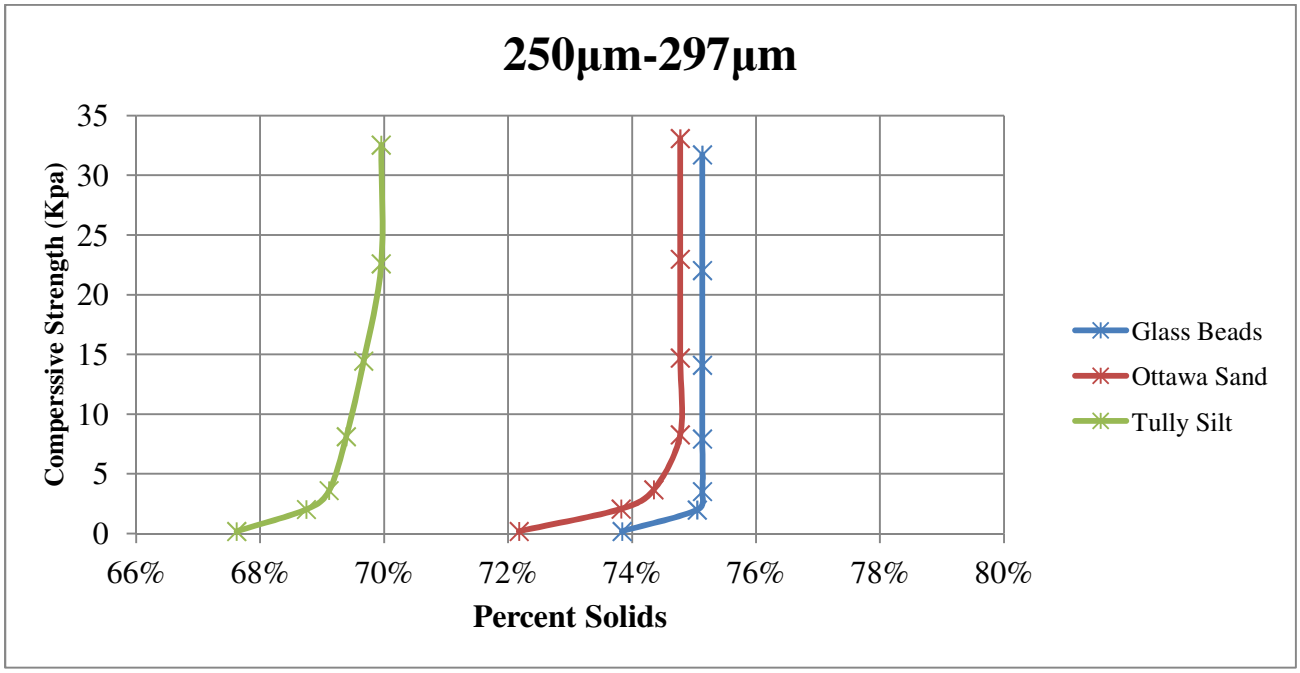

Figure 15c: *Comparison of Particle Shape Effect on Compressibility for 250µm-297µm*

For the 250µm-297µm sediment particle size range, Tully Silt (sphericity=0.63) has obtained the lowest final percent solids of approximately 70% and glass beads (sphericity=0.988) obtained the highest final percent solids of 75%. Ottawa Sand (sphericity=0.718) obtained a final percent solids in between those of the other sediment types of approximately 74.8%.

7. Discussion

The three sediments tested were examined on the basis of their particle size and particle shape. In addition, variability in test results is discussed.

7.1 *Effect of Particle Size*

The compressibility of a given sediment is related to particle size. It is important to distinguish that all materials tested are essentially incompressible, but the particle structure that they form is

compressible. For this study, the three particle size ranges used were 105μm-177μm, 177μm-250μm and 250μm-297μm. Test results indicate that the materials of smaller particle size generally exhibit greater amounts of structural compression and therefore a greater increase in percent solids. This can most clearly be seen with Tully Silt (Figures 13a, 13b and 13c). The total change in percent solids of Tully Silt 250μm-297μm is approximately 2%, whereas the change in percent solids of Tully Silt 177μm-250μm and 105μm-177μm are approximately 3.5% and 5%, respectively. Examining Ottawa Sand in the same manner, the 250μm-297μm has a change of approximately 2%, whereas the change in percent solids of Ottawa 177μm-250μm and 105μm-177μm are roughly 4% and 6% respectively (Figures 12a, 12b and 12c). These values are less pronounced in results for glass beads, where the 250μm-297μm percent solids change is 2% and the 177μm-250μm and 105μm-177μm ranges have a roughly 3% change in percent solids (Figures 11a, 11b and 11c). It is believed that sediments of smaller particle sizes have structures that are generally more compressible because there is a larger amount of void space between particles. When the number of particles is increased for the same amount of percent solids, the void ratio becomes higher, creating the opportunity for larger amounts of particle network compression from the rearrangement of particles.

Particle size does not show a strong correlation with the achievement of a material's final percent solids. For glass beads, the smallest particle size range of 105μm-177μm on average obtained a lower final percent whereas the middle particle size range of 177μm-250μm obtained the highest final percent solids on average (Figure 14a). For Ottawa Sand, the smallest particle size range of 105μm-177μm obtained the highest final percent solids on average, whereas the particles of the largest size range of 250μm-297μm obtained the lowest final percent solids on average (Figure 14b). Similarly the Tully Silt particles of the largest size range of 250μm-297μm obtained the

lowest final percent solids on average. The smallest Tully Silt particle size range of 105μm-177μm and the middle Tully Silt particle size range of 177μm-250μm on average obtained similar values of final percent solids (Figure 14c).

For Ottawa Sand, the final percent of all three particle size ranges were between 74% and 76% solids (Figures 12a, 12b and 12c) when subjected the highest compressive force whereas the initial percentage solids ranged with each sediment particle size range. The 250μm-297μm size range had an initial percent solids between 71.5%-73%, the 177μm-250μm size range had an initial percent solids between 72%-73%, and 105μm-177μm size range had an initial percent solids between 71%-72%. In contrast, the three different Tully Silt particle size ranges did not achieve similar final percent solids concentrations at the maximum compressive force (Figures 13a, 13b and 13c). The 250μm-297μm range showed a final percent solids concentration of 70% whereas the 177μm-250μm and 105μm-177μm ranges showed final percent solids concentrations of approximately 72-73%.

The compressibility of a sediment's particle structure is represented by the slope of the P_y vs percent solids curve. The curves of the Tully Silt 105μm-177μm size range (Figure 13a) most nearly resemble the relationship developed by De Kretser et al. (1997). The results show that fine, non-spherical sediments compress more gradually. In this study, compression tests on kaolinite particles were conducted, which have a diameter of 1μm-10μm, much smaller than any of the sediments tested in this study. Incompressible materials will show curves that are simply vertical lines and highly compressible materials will show gradual curves.

7.2 *Effect of Particle Shape*

Particle shape is directly correlated to packing density. It is known that perfect spheres achieve the densest possible packing structure of any shape (Farr and Groot, 2009). Spherical sediment particles can therefore achieve a greater packing density in comparison to less spherical, elongated sediment particles. Examining the percentage of solids of three materials of the same size range, the more spherical glass beads consistently show a higher initial solids content on average (Figures 15a, 15b and 15c). This indicates that when particles in the test tube were allowed to settle naturally by gravity, the glass beads achieved a denser initial packing structure than the less spherical silica and Tully silt particles. Examining the 250μm-297μm size range, glass beads showed an initial solids content of 73-74.5% (Figure 11c), Ottawa Sand obtained 72-73.5% (Figure 12c) and Tully Silt obtained roughly 68% solids (Figure 13c). Examining the 177μm-250μm size range, glass beads showed an initial solids content of 74% (Figure 11b), Ottawa Sand obtained 72-73.5% (Figure 12b) and Tully Silt obtained roughly 69% solids (Figure 13b). The same trend was seen in the 105μm-177μm size range, where glass beads showed an initial solids content of 72-73% (Figure 11a), Ottawa Sand obtained 71-72% (Figure 12a) and Tully Silt obtained roughly 66-68% solids (Figure 13a). Sediment of higher sphericity consistently achieved a higher initial solids content.

Sediment material of higher sphericity also achieves a higher final solids content. Glass beads on average show a denser maximum packing structure after the highest applied compressive force (Figure 15b and 15c), while Tully Silt shows the lowest final percent solids (Figures 15a, 15b and 15c). This is most clearly seen for the 177μm-250μm and 105μm-177μm size ranges. For example, the final percentage solids of size 177μm-250μm glass beads are 77.5% (Figure 11b), while the corresponding values for Ottawa Sand and Tully silt are roughly 75% (Figure 12b) and

73% (Figure 13b), respectively. Examining the 250μm-297μm size range, glass beads show a final solids content of 75.5% (Figure 12c), while the corresponding values for Ottawa Sand and Tully Silt are roughly 75% (Figure 11c) and 70% (Figure 13c), respectively.

Materials of varying sphericity achieve a maximum packing density at different magnitudes of compressive force. More spherical material requires a lesser compressive force to reach a state where no further compression occurs. This is because less spherical particles require more reorientation in order to reach a denser packing structure. Each successive data point on the compressibility curve indicates an increase in rotational speed and hence exerted gravitational force. More spherical sediment reaches maximum packing density at lower rotational speeds while less spherical material requires greater rotational speeds for the same effect. Size 105μm-177μm glass beads show compression up to 300 RPM and subsequently show no increase in percent solids whereas Ottawa size 105μm-177μm shows compression until 600 RPM and Tully Silt shows compression through the 800 RPM and 1000 RPM data points. The continuous compression of Tully Silt at both low and high rotational speeds is representative of the continuous reorientation of the particle network. The amount of incremental particle orientation is represented by the slope of the $P_y(\square)$ vs percent solids curve. Sediments that show more reorientation when subjected to increasing gravitational forces show curves that are more gradual. Tully size 177μm-250μm shows a curve with a gradually increasing slope, whereas the silica and glass beads of the same size range show curves that change more abruptly. This trend occurs because the less spherical Tully Silt particle network rearranges gradually with each successive compressive force to achieve the optimal packing structure.

7.3 *Data Variability*

Variability in results can be attributed to several factors regarding testing methods, equipment and material consistency. One major source of variability is the exact reading of slurry and water heights in centrifuge tubes. If the water height is slightly incorrect, the data curve will shift significantly to a higher or lower percent solids. Another possible source of data inconsistency is material variability. All sediment was thoroughly mixed prior to testing, however the polydispersions could have small differences in particle size ranges from sample to sample. The specific gravity of each sediment could also play a small role in test result variability, although the specific gravity values for all three sediments are fairly similar.

8. Conclusion

The behavior of dredged sediments in geotextile tubes is important to be able to predict the dewatering time of the geotextile tube as well as to determine the amount of slurry that can be pumped into the tube. Based on sphericity tests on more than 400 sediment particles, specific gravity determination and compression tests on all 9 sediment shape and size ranges, the following conclusions are made:

1. Sediments of smaller particle sizes have structures that are more compressible because there is a larger amount of void space between particles. When the number of particles is increased, the void ratio becomes higher, creating the opportunity for larger amounts of particle network compression.

2. More spherical sediment particles show a higher initial solids content as well as higher final solids content, indicative of the natural packing ability of the sediment

3. More spherical sediment reaches maximum packing density at lower forces while less spherical material requires greater forces for the same effect.

The stress profiles developed for various sediment particle shapes and sizes can be used to determine the percent solids for changing situations inside of a geotextile tube Given the final percent solids of a sediment, practicing engineers and geotechnical engineering researchers will be able to predict the permeability of the filter cake inside of a geotextile tube and therefore determine the dewatering time. The amount of compression that occurs for a given sediment will play a role in the determination of the final percent solids.

Literature Cited

Buscall, Richard, and Lee R. White. "The consolidation of concentrated suspensions. Part 1. The theory of sedimentation." *Journal of the Chemical Society, Faraday Transactions 1: Physical Chemistry in Condensed Phases* 83.3 (1987): 873-891.

Channell, Glenn M., and Charles F. Zukoski. "Shear and compressive rheology of aggregated alumina suspensions." *AIChE journal* 43.7 (1997): 1700-1708.

Cho, Gye-Chun, Jake Dodds, and J. Carlos Santamarina. "Particle shape effects on packing density, stiffness, and strength: natural and crushed sands." *Journal of Geotechnical and Geoenvironmental Engineering* 132.5 (2006): 591-602.

Cubrinovski, Misko, and Kenji Ishihara. "Maximum and minimum void ratio characteristics of sands." *Soils and foundations* 42.6 (2002): 65-78.

Curvers, Daan, et al. "A centrifugation method for the assessment of low pressure compressibility of particulate suspensions." *Chemical Engineering Journal* 148.2 (2009): 405-413.

De Kretser, Ross, Peter J. Scales, and David V. Boger. "Improving clay-based tailings disposal: Case study on coal tailings." *AIChE journal* 43.7 (1997): 1894-1903.

Farr R.S., Groot R.D. “Close packing density of polydisperse hard spheres”. Journal of chemical physics. Volume 131. December 2009.

Fowler, Jack, R. M. Bagby, and Ed Trainer. "Dewatering sewage sludge with geotextile tubes." *Proceedings of the 49th Canadian Geotechnical Conference*. 1996.

Gaffney, D.A. (2001). Geotextile tube dewatering: Part 1 – design parameters. *GFR Magazine*, 19, No. 7, 1-5.

Gu, Guoxing, et al. "Role of fine kaolinite clay in toluene-diluted bitumen/water emulsion." *Colloids and Surfaces A: Physicochemical and Engineering Aspects* 215.1 (2003): 141-153.

Huang, C.-C. & Luo, S.-Y. (2007). Dewatering of reservoir sediment slurry using woven geotextiles. Part I: Experimental results. Geosynthetics International, 14, No. 5, 253–263.

Janke, N. C. "Effect of shape upon the settling velocity of regular convex geometric particles." *Journal of Sedimentary Research* 36.2 (1966).

Miller, Kelly T., Renee M. Melant, and Charles F. Zukoski. "Comparison of the Compressive Yield Response of Aggregated Suspensions: Pressure Filtration, Centrifugation, and Osmotic Consolidation." *Journal of the American Ceramic Society* 79.10 (1996): 2545-556. Print.

Moo-Young, Horace K., and Wayne R. Tucker. "Testing Procedures to Assess the Viability of Dewatering with Geotextile Tubes." *Geotextiles and Geomembranes*20.3 (2002): 191-

212. *Testing Procedures to Assess the Viability of Dewatering with Geotextile Tubes*. 3 May 2002. Web. 09 Feb. 2014.

Moo-Young, Horace K., and Wayne R. Tucker. "Evaluation of vacuum filtration testing for geotextile tubes." *Geotextiles and Geomembranes* 20.3 (2002): 191-212.

Nasser, M. S., and A. E. James. "The effect of polyacrylamide charge density and molecular weight on the flocculation and sedimentation behaviour of kaolinite suspensions." *Separation and purification technology* 52.2 (2006): 241-252.

Nasser, M. S., and A. E. James. "Settling and sediment bed behaviour of kaolinite in aqueous media." *Separation and purification technology* 51.1 (2006): 10-17.

Satyamurthy, R. (2008). *Experimental investigations of geotextile tube dewatering.* (Order No. 3345019, Syracuse University). *ProQuest Dissertations and Theses*, 239. Retrieved from http://search.proquest.com/docview/304407256?accountid=14214. (304407256).

Smoltczyk, Ulrich. *Geotechnical Engineering Handbook*. Vol. 1. N.p.: John Wiley & Sons, 2002. 132. Web. 15 Feb. 2014.

"Assessment and Remediation of Contaminated Sediments (ARCS) Program." *Epa.gov*. U.S. Environmental Protection Agency, 26 June 2012. Web. 9 Feb. 2014.

U.S. EPA. "Dredged Material Management." *Www.epa.gov*. U.S. Environmental Protection Agency, 2 Nov. 2012. Web. 9 Feb. 2014.

Wadell, Hakon. "Volume, Shape, and Roundness of Rock Particles." *The Journal of Geology* 40.5 (1932): 443-51. *JSTOR*. Web. 15 Feb. 2014.

Wilson, Joe. "Overview of Corps National Dredging Program and Regulations." *USACE.army.mil*. U.S. Army Corps of Engineers, 9 May 2013. Web. 17 Apr. 2014.

Witt, K. J., and Brauns, J. (1983). “Permeability—anisotropy due to particle shape.” J. Geotech. Eng., 109(9), 1181–1187.

Appendix A

Sediment Images Used for Sphericity

Glass Beads

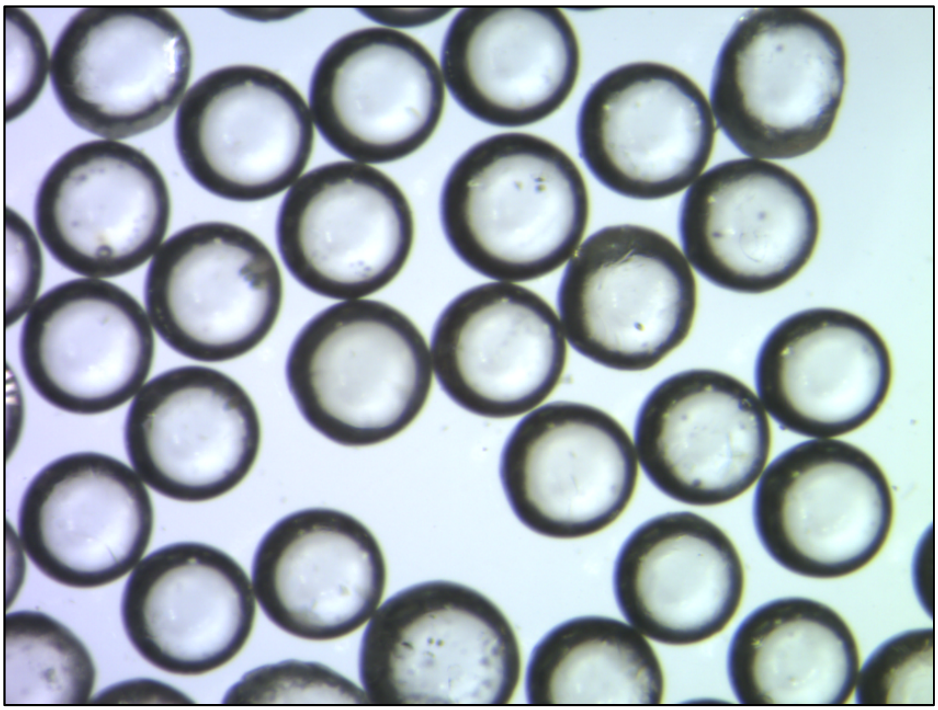

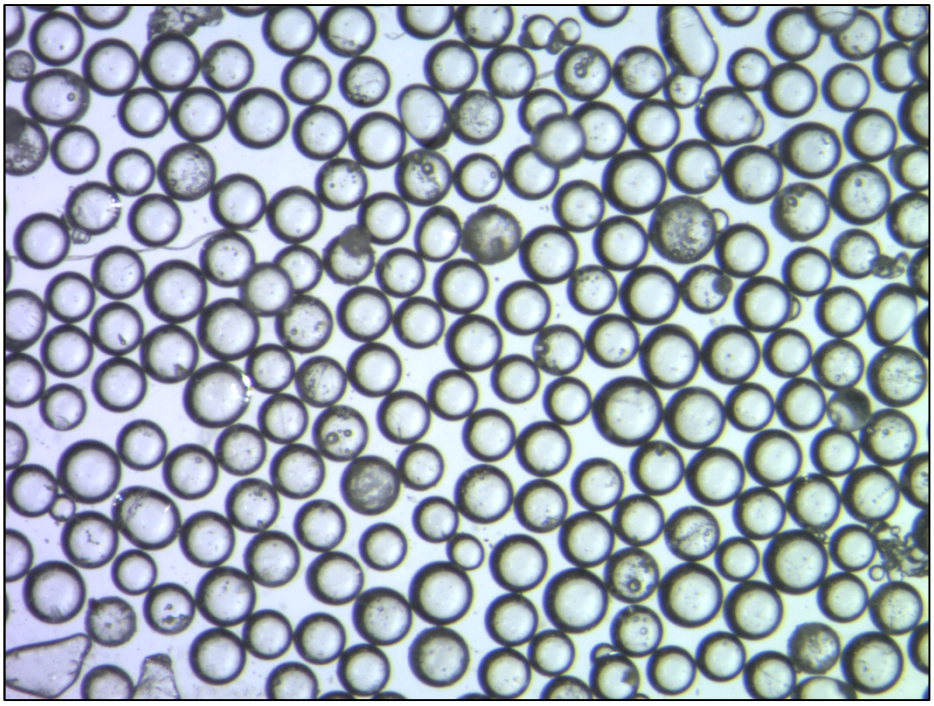

Ottawa Sand

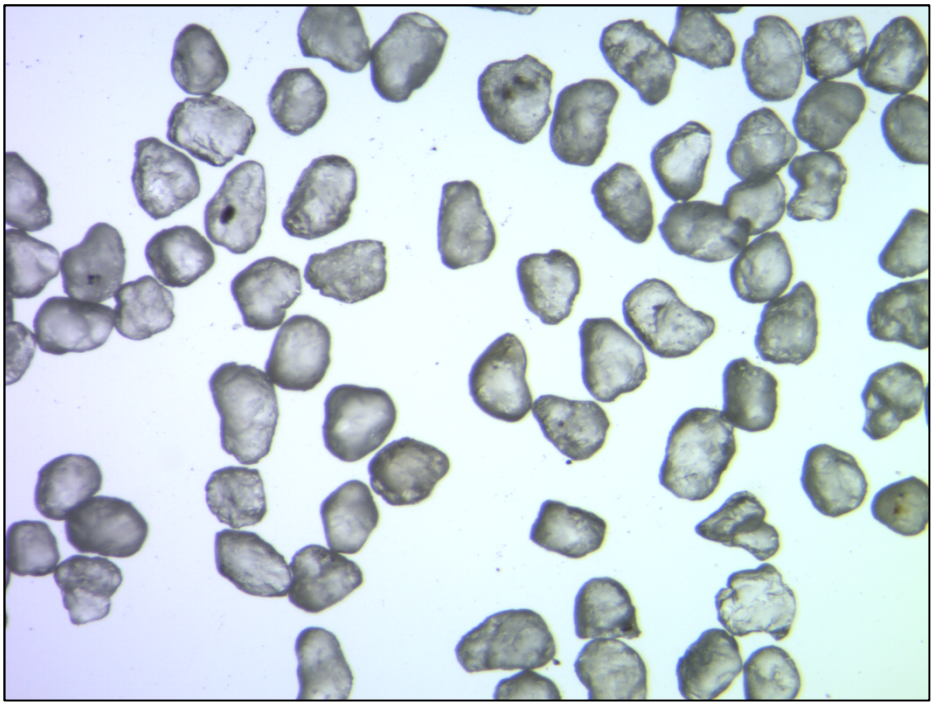

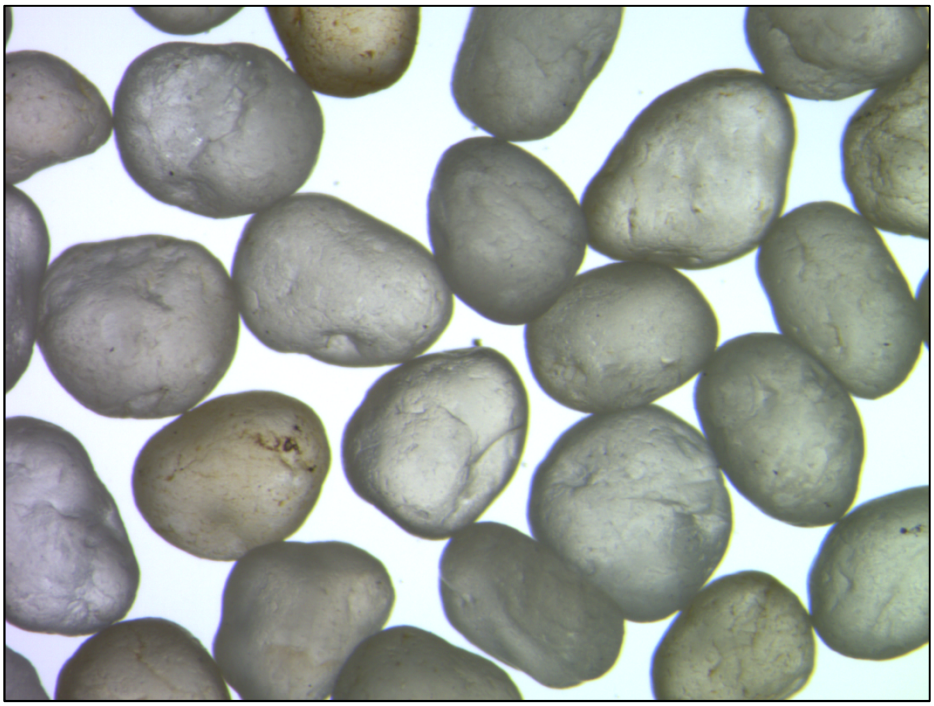

Tully Silt

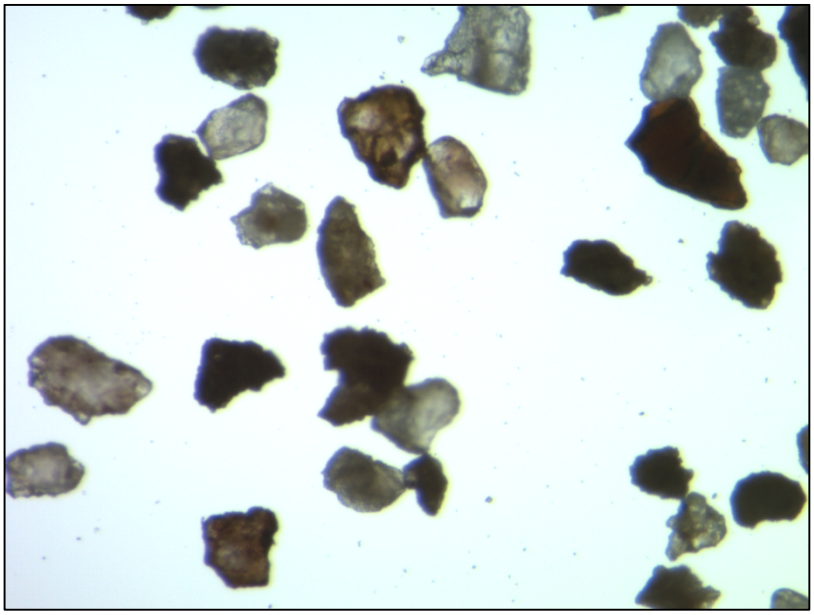

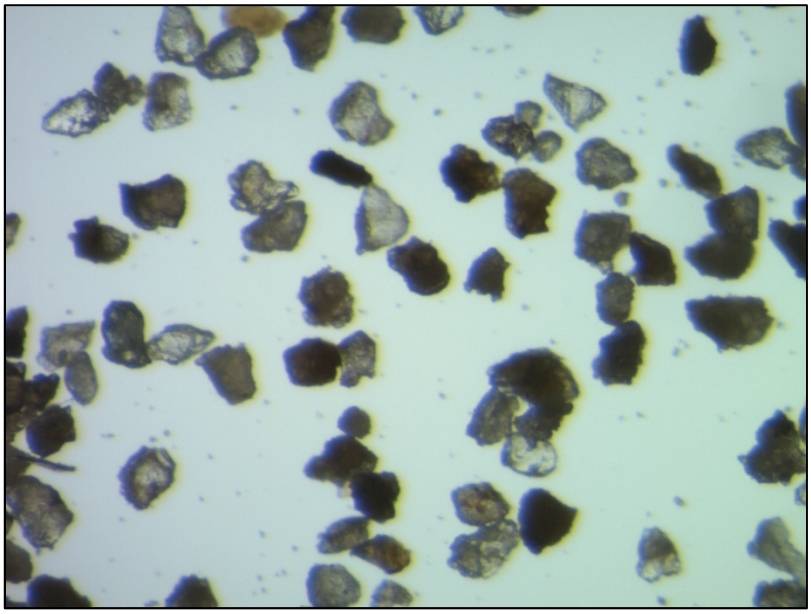

Appendix B

Sphericity Measurements

Table A: Glass Beads Sphericity Measurement size 250μm-297μm

Particle No.	D Inner (pixels)	D Outer (pixels)	Sphericity
1	0.22	0.26	0.85
2	0.25	0.26	0.96
3	0.24	0.24	1
4	0.27	0.27	1
5	0.23	0.23	1
6	0.24	0.25	0.96
7	0.29	0.29	1
8	0.25	0.25	1
9	0.26	0.265	0.98
10	0.25	0.25	1
11	0.25	0.25	1
12	0.24	0.24	1
13	0.23	0.23	1
14	0.24	0.24	1
15	0.27	0.27	1
16	0.29	0.32	0.91
17	0.27	0.275	0.98
18	0.27	0.275	0.98
19	0.23	0.23	1
20	0.26	0.26	1
21	0.27	0.27	1
22	0.28	0.285	0.98
23	0.28	0.285	0.98
24	0.29	0.29	1
25	0.29	0.29	1
26	0.27	0.27	1
27	0.275	0.275	1
28	0.27	0.27	1
29	0.22	0.22	1
30	0.24	0.24	1
31	0.3	0.3	1
32	0.25	0.25	1
33	0.25	0.25	1
34	0.25	0.255	0.98
35	0.26	0.26	1

36	0.26	0.26	1
37	0.28	0.28	1
38	0.26	0.27	0.96
39	0.28	0.29	0.97
40	0.28	0.285	0.98
41	0.29	0.29	1
42	0.25	0.25	1
43	0.25	0.25	1
44	0.27	0.27	1
45	0.27	0.27	1
46	0.27	0.285	0.95
47	0.3	0.3	1
48	0.27	0.27	1
49	0.27	0.27	1
50	0.23	0.23	1
	Average Sphericity		**0.988**

Table B: Ottawa Sand Sphericity Measurement size 250μm-297μm

Particle No.	**D Inner (pixels)**	**D Outer (pixels)**	**Sphericity**
1	100	122	0.82
2	79	149	0.53
3	95	123	0.77
4	104	147	0.71
5	111	179	0.62
6	74	115	0.64
7	146	204	0.72
8	110	183	0.60
9	107	148	0.72
10	102	179	0.57
11	134	186	0.72
12	126	180	0.70
13	161	193	0.83
14	121	143	0.85
15	134	199	0.67
16	122	151	0.81
17	146	181	0.81
18	107	158	0.68
19	64	66	0.97
20	126	203	0.62

21	177	218	0.81
22	79	100	0.79
23	73	125	0.58
24	94	154	0.61
25	127	176	0.72
26	91	130	0.70
27	124	148	0.84
28	98	115	0.85
29	63	108	0.58
30	115	177	0.65
31	106	136	0.78
32	120	152	0.79
33	118	173	0.68
34	99	136	0.73
35	133	196	0.68
36	128	181	0.71
37	80	135	0.59
38	97	131	0.74
39	161	238	0.68
40	88	135	0.65
41	76	93	0.82
42	83	140	0.59
43	98	188	0.52
44	80	123	0.65
45	68	85	0.80
46	85	90	0.94
47	97	114	0.85
48	70	117	0.60
49	67	112	0.60
50	80	136	0.59
	Average Sphericity		**0.710**

Table C: Tully Silt Sphericity Measurement size 250µm-297µm

Particle No.	**D Inner (pixels)**	**D Outer (pixels)**	**Sphericity**
1	52	71	0.73
2	41	60	0.68
3	29	58	0.50
4	38	53	0.72
5	36	51	0.71
6	31	49	0.63

7	54	83	0.65
8	46	84	0.55
9	32	53	0.60
10	36	46	0.78
11	39	56	0.70
12	36	45	0.80
13	37	56	0.66
14	34	58	0.59
15	28	49	0.57
16	58	77	0.75
17	33	63	0.52
18	36	47	0.77
19	38	59	0.64
20	76	107	0.71
21	41	54	0.76
22	57	88	0.65
23	34	65	0.52
24	44	63	0.70
25	32	50	0.64
26	38	69	0.55
27	49	77	0.64
28	47	61	0.77
29	31	67	0.46
30	32	48	0.67
31	36	58	0.62
32	58	89	0.65
33	67	91	0.74
34	34	74	0.46
35	35	53	0.66
36	33	50	0.66
37	14	148	0.09
38	44	54	0.81
39	39	61	0.64
40	50	66	0.76
41	54	77	0.70
42	34	52	0.65
43	36	55	0.65
44	36	53	0.68
45	30	50	0.60
46	31	56	0.55
47	45	89	0.51

48	74	143	0.52
49	55	93	0.59
50	38	55	0.69
	Average Sphericity		**0.637**

Table D: Ottawa Sand Sphericity Measurement size 177µm-250µm

Particle No.	**D Inner (pixels)**	**D Outer (pixels)**	**Sphericity**
1	44	74	0.59
2	61	82	0.74
3	51	76	0.67
4	56	83	0.67
5	57	74	0.77
6	51	64	0.80
7	53	76	0.70
8	42	54	0.78
9	56	83	0.67
10	48	66	0.73
11	44	67	0.66
12	56	77	0.73
13	51	62	0.82
14	69	94	0.73
15	36	49	0.73
16	41	63	0.65
17	41	61	0.67
18	54	73	0.74
19	40	72	0.56
20	45	59	0.76
21	52	90	0.58
22	58	89	0.65
23	60	66	0.91
24	61	80	0.76
25	36	39	0.92
26	39	54	0.72
27	62	87	0.71
28	65	87	0.75
29	34	40	0.85
30	47	59	0.80
31	53	72	0.74
32	52	60	0.87
33	69	96	0.72

34	64	93	0.69
35	65	86	0.76
36	44	65	0.68
37	66	72	0.92
38	51	81	0.63
39	66	97	0.68
40	44	63	0.70
41	52	65	0.80
42	67	86	0.78
43	42	58	0.72
44	41	64	0.64
45	59	77	0.77
46	53	83	0.64
47	52	64	0.81
48	72	93	0.77
49	60	85	0.71
50	73	93	0.78
	Average Sphericity		**0.733**

Table E: Tully Silt Sphericity Measurement size 177µm-250µm

Particle No.	**D Inner (pixels)**	**D Outer (pixels)**	**Sphericity**
1	128	182	0.70
2	90	141	0.64
3	96	140	0.69
4	82	130	0.63
5	80	132	0.61
6	85	122	0.70
7	96	183	0.52
8	126	182	0.69
9	105	183	0.57
10	89	151	0.59
11	113	209	0.54
12	101	150	0.67
13	88	142	0.62
14	73	105	0.70
15	78	151	0.52
16	111	222	0.50
17	91	141	0.65
18	85	124	0.69
19	124	206	0.60

20	106	148	0.72
21	94	146	0.64
22	74	139	0.53
23	85	109	0.78
24	81	137	0.59
25	79	124	0.64
26	87	166	0.52
27	85	125	0.68
28	129	161	0.80
29	87	121	0.72
30	100	154	0.65
31	110	203	0.54
32	92	133	0.69
33	79	161	0.49
34	88	174	0.51
35	90	172	0.52
36	106	267	0.40
37	78	117	0.67
38	87	147	0.59
39	97	136	0.71
40	104	168	0.62
41	82	170	0.48
42	83	125	0.66
43	98	135	0.73
44	87	113	0.77
45	128	229	0.56
46	80	124	0.65
47	69	126	0.55
48	81	152	0.53
49	69	141	0.49
50	74	131	0.56
	Average Sphericity		**0.616**

Table F: Ottawa Sand Sphericity Measurement size 105µm-177µm

Particle No.	**D Inner (pixels)**	**D Outer (pixels)**	**Sphericity**
1	36	51	0.71
2	37	58	0.64
3	31	50	0.62
4	34	51	0.67
5	33	51	0.65

6	37	43	0.86
7	44	55	0.80
8	48	61	0.79
9	46	61	0.75
10	39	64	0.61
11	30	52	0.58
12	36	60	0.60
13	52	73	0.71
14	47	65	0.72
15	51	62	0.82
16	42	70	0.60
17	53	89	0.60
18	39	42	0.93
19	53	70	0.76
20	40	63	0.63
21	42	61	0.69
22	38	52	0.73
23	45	62	0.73
24	60	83	0.72
25	49	80	0.61
26	53	73	0.73
27	37	48	0.77
28	47	60	0.78
29	34	45	0.76
30	32	36	0.89
31	39	50	0.78
32	36	56	0.64
33	41	56	0.73
34	44	61	0.72
35	35	49	0.71
36	49	59	0.83
37	43	58	0.74
38	38	57	0.67
39	39	64	0.61
40	55	74	0.74
41	50	83	0.60
42	53	82	0.65
43	38	60	0.63
44	43	66	0.65
45	44	64	0.69
46	53	72	0.74

47	54	77	0.70
48	53	66	0.80
49	46	62	0.74
50	50	64	0.78
	Average Sphericity		**0.712**

Table G: Ottawa Sand Sphericity Measurement size 105µm-177µm

Particle No.	**D Inner (pixels)**	**D Outer (pixels)**	**Sphericity**
1	86	119	0.72
2	118	189	0.62
3	113	186	0.61
4	105	159	0.66
5	64	149	0.43
6	79	135	0.59
7	64	153	0.42
8	89	203	0.44
9	98	212	0.46
10	123	227	0.54
11	97	154	0.63
12	110	168	0.65
13	87	137	0.64
14	59	72	0.82
15	72	114	0.63
16	66	84	0.79
17	72	114	0.63
18	73	120	0.61
19	70	115	0.61
20	89	225	0.40
21	57	73	0.78
22	84	108	0.78
23	95	162	0.59
24	72	122	0.59
25	80	146	0.55
26	69	99	0.70
27	55	80	0.69
28	44	114	0.39
29	88	111	0.79
30	101	166	0.61
31	98	157	0.62
32	85	120	0.71

33	116	177	0.66
34	75	104	0.72
35	86	128	0.67
36	101	145	0.70
37	59	83	0.71
38	84	129	0.65
39	74	113	0.65
40	98	129	0.76
41	64	90	0.71
42	58	130	0.45
43	74	118	0.63
44	85	108	0.79
45	93	109	0.85
46	93	138	0.67
47	60	141	0.43
48	96	122	0.79
49	73	114	0.64
50	86	116	0.74
	Average Sphericity		**0.638**

Appendix C

Centrifuge Compressibility Data

Soil:	Glass 250µm-297µm	(#)	**Specific Gravity:**	2.48	(#)						
Percent Solids:	33.00	(%)	**Density water:**	1.00	(gm/cm^3)						
Radius:	12.00	(cm)	**Volume Fraction:**	0.17							
Mass solid:	16.50	(gm)									
Mass water:	33.50	(gm)	**Slope S:**	-0.0177	(from plot)						
						Tube #1					
Time (min)	**RPM:**	**Acceleration (cm/s^2):**	**Gravity:**	**ln (g):**	**Tube Height:**	**Height(cm):**	**Change in Tube Height**	**% Change in Tube Height**	**Py (kPa)**	**Φ**	**Ps (%)**
					37.3	**8.3**					
0	0.00	981.00	1.00	0.00	31.67	2.67			0.18	0.52	73%
60	300.00	10800.00	11.01	2.40	31.52	2.52	0.15	6%	1.97	0.55	75%
120	400.00	19200.00	19.58	2.97	31.5	2.5	0.02	1%	3.51	0.55	75%
180	600.00	43200.00	44.05	3.79	31.5	2.5	0	0%	7.89	0.55	75%
240	800.00	76800.00	78.31	4.36	31.5	2.5	0	0%	14.02	0.55	75%
300	1000.00	120000.00	122.37	4.81	31.5	2.5	0	0%	21.91	0.55	75%
360	1200.00	172800.00	176.21	5.17	31.5	2.5	0	0%	31.55	0.55	75%
										0.39	
Soil:	Glass 250µm-297µm	(#)	**Specific Gravity:**	2.48	(#)						
Percent Solids:	33.00	(%)	**Density water:**	1.00	(gm/cm^3)						
Radius:	12.00	(cm)	**Volume Fraction:**	0.17							
Mass solid:	16.50	(gm)									
Mass water:	33.50	(gm)	**Slope S:**	-0.0223	(from plot)						
						Tube #2					
Time (min)	**RPM:**	**Acceleration (cm/s^2):**	**Gravity:**	**ln (g):**	**Tube Height:**	**Height(cm):**	**Change in Tube Height**	**% Change in Tube Height**	**Py (kPa)**	**Φ**	**Ps (%)**
					51.3	**8.3**					
0	0.00	981.00	1.00	6.89	45.6	2.6			0.18	0.53	74%
60	300.00	10800.00	11.01	2.40	45.5	2.5	0.1	4%	1.97	0.55	75%
120	400.00	19200.00	19.58	2.97	45.5	2.5	0	0	3.51	0.55	75%
180	600.00	43200.00	44.05	3.79	45.5	2.5	0	0	7.89	0.55	75%
240	800.00	76800.00	78.31	4.36	45.5	2.5	0	0	14.02	0.55	75%
300	1000.00	120000.00	122.37	4.81	45.5	2.5	0	0	21.91	0.55	75%
360	1200.00	172800.00	176.21	5.17	45.5	2.5	0	0	31.55	0.55	75%
										0.39	
Soil:	Glass 250µm-297µm	(#)	**Specific Gravity:**	2.48	(#)						
Percent Solids:	33.00	(%)	**Density water:**	1.00	(gm/cm^3)						
Radius:	12.00	(cm)	**Volume Fraction:**	0.17							
Mass solid:	16.50	(gm)									
Mass water:	33.50	(gm)	**Slope S:**	-0.0089	(from plot)						
						Tube #3					
Time (min)	**RPM:**	**Acceleration (cm/s^2):**	**Gravity:**	**ln (g):**	**Tube Height:**	**Height(cm):**	**Change in Tube Height**	**% Change in Tube Height**	**Py (kPa)**	**Φ**	**Ps (%)**
					60.38	**8.38**					
0	0.00	981.00	1.00	0.00	54.6	2.6			0.18	0.54	74%
60	300.00	10800.00	11.01	2.40	54.6	2.6	0	0%	1.98	0.54	74%
120	400.00	19200.00	19.58	2.97	54.6	2.6	0	0%	3.52	0.54	74%
180	600.00	43200.00	44.05	3.79	54.6	2.6	0	0%	7.93	0.54	74%
240	800.00	76800.00	78.31	4.36	54.6	2.6	0	0%	14.09	0.54	74%
300	1000.00	120000.00	122.37	4.81	54.6	2.6	0	0%	22.02	0.54	74%
360	1200.00	172800.00	176.21	5.17	54.6	2.6	0	0%	31.71	0.54	74%
										0.37	
Soil:	Glass 250µm-297µm	(#)	**Specific Gravity:**	2.48	(#)						
Percent Solids:	33.00	(%)	**Density water:**	1.00	(gm/cm^3)						
Radius:	12.00	(cm)	**Volume Fraction:**	0.17							
Mass solid:	16.50	(gm)									
Mass water:	33.50	(gm)	**Slope S:**	-0.0089	(from plot)						
						Tube #4					
Time (min)	**RPM:**	**Acceleration (cm/s^2):**	**Gravity:**	**ln (g):**	**Tube Height:**	**Height(cm):**	**Change in Tube Height**	**% Change in Tube Height**	**Py (kPa)**	**Φ**	**Ps (%)**
					48.45	**8.45**					
0	0.00	981.00	1.00	0.00	42.6	2.6			0.18	0.54	75%
60	300.00	10800.00	11.01	2.40	42.55	2.55	0.05	2%	2.00	0.55	75%
120	400.00	19200.00	19.58	2.97	42.55	2.55	0	0%	3.56	0.55	75%
180	600.00	43200.00	44.05	3.79	42.55	2.55	0	0%	8.01	0.55	75%
240	800.00	76800.00	78.31	4.36	42.55	2.55	0	0%	14.24	0.55	75%
300	1000.00	120000.00	122.37	4.81	42.55	2.55	0	0%	22.25	0.55	75%
360	1200.00	172800.00	176.21	5.17	42.55	2.55	0	0%	32.05	0.55	75%
										0.39	

Soil:	Glass 177µm-250µm	(#)	Specific Gravity:	2.46	(#)
Percent Solids:	33.00	(%)	Density water:	1.00	(gm/cm^3)
Radius:	12.00	(cm)	Volume Fraction:	0.17	
Mass solid:	16.50	(gm)			
Mass water:	33.50	(gm)	Slope S:	-0.038	(from plot)

Tube #1

Time (min)	RPM:	Acceleration (cm/s^2):	Gravity:	ln (g):	Tube Height: 28.2	Height(cm): 8.2	Change in Tube Height	% Change in Tube Height	Py (kPa)	ϕ	Ps (%)
0	0.00	981.00	1.00	0.00	22.5	2.5			0.18	0.56	75%
60	300.00	10800.00	11.01	2.40	22.35	2.35	0.15	6%	1.95	0.59	78%
120	400.00	19200.00	19.58	2.97	22.3	2.3	0.05	2%	3.47	0.60	79%
180	600.00	43200.00	44.05	3.79	22.3	2.3	0	0%	7.81	0.60	79%
240	800.00	76800.00	78.31	4.36	22.3	2.3	0	0%	13.88	0.60	79%
300	1000.00	120000.00	122.37	4.81	22.3	2.3	0	0%	21.68	0.60	79%
360	1200.00	172800.00	176.21	5.17	22.3	2.3	0	0%	31.23	0.60	79%
										0.44	

Soil:	Glass 177µm-250µm	(#)	Specific Gravity:	2.46	(#)
Percent Solids:	33.00	(%)	Density water:	1.00	(gm/cm^3)
Radius:	12.00	(cm)	Volume Fraction:	0.17	
Mass solid:	16.50	(gm)			
Mass water:	33.50	(gm)	Slope S:	-0.0355	(from plot)

Tube #2

Time (min)	RPM:	Acceleration (cm/s^2):	Gravity:	ln (g):	Tube Height: 37.4	Height(cm): 8.4	Change in Tube Height	% Change in Tube Height	Py (kPa)	ϕ	Ps (%)
0	0.00	981.00	1.00	0.00	31.65	2.65			0.18	0.54	74%
60	300.00	10800.00	11.01	2.40	31.45	2.45	0.2	8%	1.99	0.58	77%
120	400.00	19200.00	19.58	2.97	31.45	2.45	0	0	3.53	0.58	77%
180	600.00	43200.00	44.05	3.79	31.45	2.45	0	0	7.94	0.58	77%
240	800.00	76800.00	78.31	4.36	31.45	2.45	0	0	14.12	0.58	77%
300	1000.00	120000.00	122.37	4.81	31.45	2.45	0	0	22.06	0.58	77%
360	1200.00	172800.00	176.21	5.17	31.45	2.45	0	0	31.77	0.58	77%
										0.41	

Soil:	Glass 177µm-250µm	(#)	Specific Gravity:	2.46	(#)
Percent Solids:	33.00	(%)	Density water:	1.00	(gm/cm^3)
Radius:	12.00	(cm)	Volume Fraction:	0.17	
Mass solid:	16.50	(gm)			
Mass water:	33.50	(gm)	Slope S:	-0.0355	(from plot)

Tube #3

Time (min)	RPM:	Acceleration (cm/s^2):	Gravity:	ln (g):	Tube Height: 69.3	Height(cm): 8.3	Change in Tube Height	% Change in Tube Height	Py (kPa)	ϕ	Ps (%)
0	0.00	981.00	1.00	0.00	63.6	2.6			0.18	0.54	74%
60	300.00	10800.00	11.01	2.40	63.4	2.4	0.2	8%	1.97	0.59	78%
120	400.00	19200.00	19.58	2.97	63.4	2.4	0	0%	3.50	0.59	78%
180	600.00	43200.00	44.05	3.79	63.4	2.4	0	0%	7.87	0.59	78%
240	800.00	76800.00	78.31	4.36	63.4	2.4	0	0%	13.98	0.59	78%
300	1000.00	120000.00	122.37	4.81	63.4	2.4	0	0%	21.85	0.59	78%
360	1200.00	172800.00	176.21	5.17	63.4	2.4	0	0%	31.46	0.59	78%
										0.42	

Soil:	Glass 177µm-250µm	(#)	Specific Gravity:	2.46	(#)
Percent Solids:	33.00	(%)	Density water:	1.00	(gm/cm^3)
Radius:	12.00	(cm)	Volume Fraction:	0.17	
Mass solid:	16.50	(gm)			
Mass water:	33.50	(gm)	Slope S:	4.00E-16	(from plot)

Tube #4

Time (min)	RPM:	Acceleration (cm/s^2):	Gravity:	ln (g):	Tube Height: 70.3	Height(cm): 8.3	Change in Tube Height	% Change in Tube Height	Py (kPa)	ϕ	Ps (%)
0	0.00	981.00	1.00	0.00	64.4	2.4			0.18	0.58	78%
60	300.00	10800.00	11.01	2.40	64.4	2.4	0	0%	1.97	0.58	78%
120	400.00	19200.00	19.58	2.97	64.4	2.4	0	0%	3.50	0.58	78%
180	600.00	43200.00	44.05	3.79	64.4	2.4	0	0%	7.87	0.58	78%
240	800.00	76800.00	78.31	4.36	64.4	2.4	0	0%	13.98	0.58	78%
300	1000.00	120000.00	122.37	4.81	64.4	2.4	0	0%	21.85	0.58	78%
360	1200.00	172800.00	176.21	5.17	64.4	2.4	0	0%	31.46	0.58	78%
										0.42	

Soil:	Glass 105µm-177µm	(#)	**Specific Gravity:**	2.74	(#)						
Percent Solids:	33.00	(%)	**Density water:**	1.00	(gm/cm^3)						
Radius:	12.00	(cm)	**Volume Fraction:**	0.15							
Mass solid:	16.50	(gm)									
Mass water:	33.50	(gm)	**Slope S:**	-0.0335	(from plot)						

Tube #1

Time (min)	RPM:	Acceleration (cm/s^2):	Gravity:	ln (g):	Tube Height: 37.5	Height(cm): 8.5	Change in Tube Height	% Change in Tube Height	Py (kPa)	ϕ	Ps (%)
0	0.00	981.00	1.00	0.00	31.7	2.7			0.20	0.49	72%
60	300.00	10800.00	11.01	2.40	31.55	2.55	0.15	6%	2.18	0.51	74%
120	400.00	19200.00	19.58	2.97	31.52	2.52	0.03	1%	3.87	0.52	75%
180	600.00	43200.00	44.05	3.79	31.52	2.52	0	0%	8.71	0.52	75%
240	800.00	76800.00	78.31	4.36	31.52	2.52	0	0%	15.49	0.52	75%
300	1000.00	120000.00	122.37	4.81	31.52	2.52	0	0%	24.20	0.52	75%
360	1200.00	172800.00	176.21	5.17	31.52	2.52	0	0%	34.85	0.52	75%
										0.37	

Soil:	Glass 105µm-177µm	(#)	**Specific Gravity:**	2.74	(#)
Percent Solids:	33.00	(%)	**Density water:**	1.00	(gm/cm^3)
Radius:	12.00	(cm)	**Volume Fraction:**	0.15	
Mass solid:	16.50	(gm)			
Mass water:	33.50	(gm)	**Slope S:**	-0.0298	(from plot)

Tube #2

Time (min)	RPM:	Acceleration (cm/s^2):	Gravity:	ln (g):	Tube Height: 51.4	Height(cm): 8.4	Change in Tube Height	% Change in Tube Height	Py (kPa)	ϕ	Ps (%)
0	0.00	981.00	1.00	0.00	45.7	2.7			0.19	0.48	72%
60	300.00	10800.00	11.01	2.40	45.6	2.6	0.1	4%	2.14	0.50	73%
120	400.00	19200.00	19.58	2.97	45.58	2.58	0.02	0.007407407	3.82	0.50	73%
180	600.00	43200.00	44.05	3.79	45.55	2.55	0.03	0.011111111	8.60	0.51	74%
240	800.00	76800.00	78.31	4.36	45.55	2.55	0	0	15.29	0.51	74%
300	1000.00	120000.00	122.37	4.81	45.55	2.55	0	0	23.88	0.51	74%
360	1200.00	172800.00	176.21	5.17	45.55	2.55	0	0	34.39	0.51	74%
										0.36	

Soil:	Glass 105µm-177µm	(#)	**Specific Gravity:**	2.74	(#)
Percent Solids:	33.00	(%)	**Density water:**	1.00	(gm/cm^3)
Radius:	12.00	(cm)	**Volume Fraction:**	0.15	
Mass solid:	16.50	(gm)			
Mass water:	33.50	(gm)	**Slope S:**	-0.0223	(from plot)

Tube #3

Time (min)	RPM:	Acceleration (cm/s^2):	Gravity:	ln (g):	Tube Height: 60.4	Height(cm): 8.4	Change in Tube Height	% Change in Tube Height	Py (kPa)	ϕ	Ps (%)
0	0.00	981.00	1.00	0.00	54.7	2.7			0.19	0.48	72%
60	300.00	10800.00	11.01	2.40	54.6	2.6	0.1	4%	2.14	0.50	73%
120	400.00	19200.00	19.58	2.97	54.58	2.58	0.02	1%	3.82	0.50	73%
180	600.00	43200.00	44.05	3.79	54.58	2.58	0	0%	8.59	0.50	73%
240	800.00	76800.00	78.31	4.36	54.58	2.58	0	0%	15.26	0.50	73%
300	1000.00	120000.00	122.37	4.81	54.58	2.58	0	0%	23.85	0.50	73%
360	1200.00	172800.00	176.21	5.17	54.58	2.58	0	0%	34.35	0.50	73%
										0.35	

Soil:	Glass 105µm-177µm	(#)	**Specific Gravity:**	2.74	(#)
Percent Solids:	33.00	(%)	**Density water:**	1.00	(gm/cm^3)
Radius:	12.00	(cm)	**Volume Fraction:**	0.15	
Mass solid:	16.50	(gm)			
Mass water:	33.50	(gm)	**Slope S:**	-0.0266	(from plot)

Tube #4

Time (min)	RPM:	Acceleration (cm/s^2):	Gravity:	ln (g):	Tube Height: 48.35	Height(cm): 8.35	Change in Tube Height	% Change in Tube Height	Py (kPa)	ϕ	Ps (%)
0	0.00	981.00	1.00	0.00	42.68	2.68			0.19	0.48	72%
60	300.00	10800.00	11.01	2.40	42.6	2.6	0.08	3%	2.13	0.50	73%
120	400.00	19200.00	19.58	2.97	42.58	2.58	0.02	1%	3.79	0.50	73%
180	600.00	43200.00	44.05	3.79	42.58	2.58	0	0%	8.54	0.50	73%
240	800.00	76800.00	78.31	4.36	42.58	2.58	0	0%	15.17	0.50	73%
300	1000.00	120000.00	122.37	4.81	42.58	2.58	0	0%	23.71	0.50	73%
360	1200.00	172800.00	176.21	5.17	42.58	2.58	0	0%	34.14	0.50	73%
										0.35	

Soil:	Tully 250µm-297µm	(#)	**Specific Gravity:**	2.62	(#)						
Percent Solids:	33.00	(%)	**Density water:**	1.00	(gm/cm^3)						
Radius:	12.00	(cm)	**Volume Fraction:**	0.16							
Mass solid:	16.50	(gm)									
Mass water:	33.50	(gm)	**Slope S:**	-0.0342	(from plot)						

Tube #1

Time (min)	RPM:	Acceleration (cm/s^2):	Gravity:	ln (g):	Tube Height: 37.3	Height(cm): 8.3	Change in Tube Height	% Change in Tube Height	Py (kPa)	ϕ	Ps (%)
0	0.00	981.00	1.00	0.00	32	3			0.18	0.44	68%
60	300.00	10800.00	11.01	2.40	31.9	2.9	0.1	3%	2.02	0.46	69%
120	400.00	19200.00	19.58	2.97	31.89	2.89	0.01	0%	3.60	0.46	69%
180	600.00	43200.00	44.05	3.79	31.87	2.87	0.02	1%	8.10	0.46	69%
240	800.00	76800.00	78.31	4.36	31.85	2.85	0.02	1%	14.42	0.47	70%
300	1000.00	120000.00	122.37	4.81	31.82	2.82	0.03	1%	22.56	0.47	70%
360	1200.00	172800.00	176.21	5.17	31.82	2.82	0	0%	32.49	0.47	70%
										0.31	

Soil:	Tully 250µm-297µm	(#)	**Specific Gravity:**	2.62	(#)						
Percent Solids:	33.00	(%)	**Density water:**	1.00	(gm/cm^3)						
Radius:	12.00	(cm)	**Volume Fraction:**	0.16							
Mass solid:	16.50	(gm)									
Mass water:	33.50	(gm)	**Slope S:**	-0.0504	(from plot)						

Tube #2

Time (min)	RPM:	Acceleration (cm/s^2):	Gravity:	ln (g):	Tube Height: 51.3	Height(cm): 8.3	Change in Tube Height	% Change in Tube Height	Py (kPa)	ϕ	Ps (%)
0	0.00	981.00	1.00	0.00	46	3			0.18	0.44	68%
60	300.00	10800.00	11.01	2.40	45.85	2.85	0.15	5%	2.03	0.47	70%
120	400.00	19200.00	19.58	2.97	45.8	2.8	0.05	0.016666667	3.61	0.47	70%
180	600.00	43200.00	44.05	3.79	45.75	2.75	0.05	0.016666667	8.15	0.48	71%
240	800.00	76800.00	78.31	4.36	45.75	2.75	0	0	14.49	0.48	71%
300	1000.00	120000.00	122.37	4.81	45.75	2.75	0	0	22.63	0.48	71%
360	1200.00	172800.00	176.21	5.17	45.75	2.75	0	0	32.59	0.48	71%
										0.33	

Soil:	Tully 250µm-297µm	(#)	**Specific Gravity:**	2.62	(#)						
Percent Solids:	33.00	(%)	**Density water:**	1.00	(gm/cm^3)						
Radius:	12.00	(cm)	**Volume Fraction:**	0.16							
Mass solid:	16.50	(gm)									
Mass water:	33.50	(gm)	**Slope S:**	-0.0322	(from plot)						

Tube #3

Time (min)	RPM:	Acceleration (cm/s^2):	Gravity:	ln (g):	Tube Height: 60.35	Height(cm): 8.35	Change in Tube Height	% Change in Tube Height	Py (kPa)	ϕ	Ps (%)
0	0.00	981.00	1.00	0.00	55	3			0.18	0.44	68%
60	300.00	10800.00	11.01	2.40	54.95	2.95	0.05	2%	2.03	0.45	68%
120	400.00	19200.00	19.58	2.97	54.9	2.9	0.05	2%	3.62	0.46	69%
180	600.00	43200.00	44.05	3.79	54.87	2.87	0.03	1%	8.15	0.47	70%
240	800.00	76800.00	78.31	4.36	54.85	2.85	0.02	1%	14.50	0.47	70%
300	1000.00	120000.00	122.37	4.81	54.85	2.85	0	0%	22.66	0.47	70%
360	1200.00	172800.00	176.21	5.17	54.85	2.85	0	0%	32.63	0.47	70%
										0.31	

Soil:	Tully 250µm-297µm	(#)	**Specific Gravity:**	2.62	(#)						
Percent Solids:	33.00	(%)	**Density water:**	1.00	(gm/cm^3)						
Radius:	12.00	(cm)	**Volume Fraction:**	0.16							
Mass solid:	16.50	(gm)									
Mass water:	33.50	(gm)	**Slope S:**	-3.43E-02	(from plot)						

Tube #4

Time (min)	RPM:	Acceleration (cm/s^2):	Gravity:	ln (g):	Tube Height: 48.3	Height(cm): 8.3	Change in Tube Height	% Change in Tube Height	Py (kPa)	ϕ	Ps (%)
0	0.00	981.00	1.00	0.00	43	3			0.18	0.44	68%
60	300.00	10800.00	11.01	2.40	42.9	2.9	0.1	3%	2.02	0.46	69%
120	400.00	19200.00	19.58	2.97	42.88	2.88	0.02	1%	3.60	0.46	69%
180	600.00	43200.00	44.05	3.79	42.87	2.87	0.01	0%	8.10	0.46	69%
240	800.00	76800.00	78.31	4.36	42.85	2.85	0.02	1%	14.42	0.47	70%
300	1000.00	120000.00	122.37	4.81	42.82	2.82	0.03	1%	22.56	0.47	70%
360	1200.00	172800.00	176.21	5.17	42.82	2.82	0	0%	32.49	0.47	70%
										0.31	

Soil:	Tully 177µm-250µm	(#)	Specific Gravity:	2.73	(#)	n					
Percent Solids:	33.00	(%)	Density water:	1.00	(gm/cm^3)						
Radius:	12.00	(cm)	Volume Fraction:	0.15							
Mass solid:	16.50	(gm)									
Mass water:	33.50	(gm)	Slope S:	-0.0591	(from plot)						

Tube #1

Time (min)	RPM:	Acceleration (cm/s^2):	Gravity:	ln (g):	Tube Height: 28.1	Height(cm): 8.1	Change in Tube Height	% Change in Tube Height	Py (kPa)	Φ	Ps (%)
0	0.00	981.00	1.00	0.00	22.8	2.8			0.19	0.45	69%
60	300.00	10800.00	11.01	2.40	22.7	2.7	0.1	4%	2.05	0.47	71%
120	400.00	19200.00	19.58	2.97	22.6	2.6	0.1	4%	3.67	0.49	72%
180	600.00	43200.00	44.05	3.79	22.55	2.55	0.05	2%	8.27	0.50	73%
240	800.00	76800.00	78.31	4.36	22.55	2.55	0	0%	14.70	0.50	73%
300	1000.00	120000.00	122.37	4.81	22.52	2.52	0.03	1%	23.00	0.50	73%
360	1200.00	172800.00	176.21	5.17	22.51	2.51	0.01	0%	33.13	0.51	74%
										0.35	

Soil:	Tully 177µm-250µm	(#)	Specific Gravity:	2.73	(#)
Percent Solids:	33.00	(%)	Density water:	1.00	(gm/cm^3)
Radius:	12.00	(cm)	Volume Fraction:	0.15	
Mass solid:	16.50	(gm)			
Mass water:	33.50	(gm)	Slope S:	-0.0504	(from plot)

Tube #2

Time (min)	RPM:	Acceleration (cm/s^2):	Gravity:	ln (g):	Tube Height: 37.15	Height(cm): 8.15	Change in Tube Height	% Change in Tube Height	Py (kPa)	Φ	Ps (%)
0	0.00	981.00	1.00	0.00	31.85	2.85			0.19	0.45	69%
60	300.00	10800.00	11.01	2.40	31.7	2.7	0.15	5%	2.07	0.47	71%
120	400.00	19200.00	19.58	2.97	31.65	2.65	0.05	0.01754386	3.68	0.48	72%
180	600.00	43200.00	44.05	3.79	31.6	2.6	0.05	0.01754386	8.30	0.49	72%
240	800.00	76800.00	78.31	4.36	31.6	2.6	0	0	14.75	0.49	72%
300	1000.00	120000.00	122.37	4.81	31.6	2.6	0	0	23.05	0.49	72%
360	1200.00	172800.00	176.21	5.17	31.6	2.6	0	0	33.20	0.49	72%
										0.34	

Soil:	Tully 177µm-250µm	(#)	Specific Gravity:	2.73	(#)
Percent Solids:	33.00	(%)	Density water:	1.00	(gm/cm^3)
Radius:	12.00	(cm)	Volume Fraction:	0.15	
Mass solid:	16.50	(gm)			
Mass water:	33.50	(gm)	Slope S:	-0.0529	(from plot)

Tube #3

Time (min)	RPM:	Acceleration (cm/s^2):	Gravity:	ln (g):	Tube Height: 69.15	Height(cm): 8.15	Change in Tube Height	% Change in Tube Height	Py (kPa)	Φ	Ps (%)
0	0.00	981.00	1.00	0.00	63.85	2.85			0.19	0.45	69%
60	300.00	10800.00	11.01	2.40	63.7	2.7	0.15	5%	2.07	0.47	71%
120	400.00	19200.00	19.58	2.97	63.6	2.6	0.1	4%	3.69	0.49	72%
180	600.00	43200.00	44.05	3.79	63.6	2.6	0	0%	8.30	0.49	72%
240	800.00	76800.00	78.31	4.36	63.6	2.6	0	0%	14.75	0.49	72%
300	1000.00	120000.00	122.37	4.81	63.58	2.58	0.02	1%	23.07	0.49	73%
360	1200.00	172800.00	176.21	5.17	63.58	2.58	0	0%	33.23	0.49	73%
										0.34	

Soil:	Tully 177µm-250µm	(#)	Specific Gravity:	2.73	(#)
Percent Solids:	33.00	(%)	Density water:	1.00	(gm/cm^3)
Radius:	12.00	(cm)	Volume Fraction:	0.15	
Mass solid:	16.50	(gm)			
Mass water:	33.50	(gm)	Slope S:	-0.0553	(from plot)

Tube #4

Time (min)	RPM:	Acceleration (cm/s^2):	Gravity:	ln (g):	Tube Height: 70.2	Height(cm): 8.2	Change in Tube Height	% Change in Tube Height	Py (kPa)	Φ	Ps (%)
0	0.00	981.00	1.00	0.00	64.8	2.8			0.19	0.46	70%
60	300.00	10800.00	11.01	2.40	64.7	2.7	0.1	4%	2.08	0.47	71%
120	400.00	19200.00	19.58	2.97	64.6	2.6	0.1	4%	3.71	0.49	73%
180	600.00	43200.00	44.05	3.79	64.6	2.6	0	0%	8.35	0.49	73%
240	800.00	76800.00	78.31	4.36	64.55	2.55	0.05	2%	14.88	0.50	73%
300	1000.00	120000.00	122.37	4.81	64.53	2.53	0.02	1%	23.27	0.51	74%
360	1200.00	172800.00	176.21	5.17	64.53	2.53	0	0%	33.51	0.51	74%
										0.35	

Soil:	Tully 105µm-177µm	(#)	**Specific Gravity:**	2.66	(#)						
Percent Solids:	33.00	(%)	**Density water:**	1.00	(gm/cm^3)						
Radius:	12.00	(cm)	**Volume Fraction:**	0.16							
Mass solid:	16.50	(gm)									
Mass water:	33.50	(gm)	**Slope S:**	-0.0628	(from plot)						

Tube #1

Time (min)	RPM:	Acceleration (cm/s^2):	Gravity:	ln (g):	Tube Height:	Height(cm):	Change in	% Change in	Py (kPa)	ϕ	Ps
					6.2	8.2	Tube Height	Tube Height			(%)
0	0.00	981.00	1.00	0.00	0.9	2.9			0.18	0.45	69%
60	300.00	10800.00	11.01	2.40	0.75	2.75	0.15	5%	2.04	0.48	71%
120	400.00	19200.00	19.58	2.97	0.7	2.7	0.05	2%	3.63	0.49	72%
180	600.00	43200.00	44.05	3.79	0.6	2.6	0.1	3%	8.20	0.50	73%
240	800.00	76800.00	78.31	4.36	0.6	2.6	0	0%	14.58	0.50	73%
300	1000.00	120000.00	122.37	4.81	0.6	2.6	0	0%	22.78	0.50	73%
360	1200.00	172800.00	176.21	5.17	0.6	2.6	0	0%	32.81	0.50	73%
										0.35	

Soil:	Tully 105µm-177µm	(#)	**Specific Gravity:**	2.66	(#)						
Percent Solids:	33.00	(%)	**Density water:**	1.00	(gm/cm^3)						
Radius:	12.00	(cm)	**Volume Fraction:**	0.16							
Mass solid:	16.50	(gm)									
Mass water:	33.50	(gm)	**Slope S:**	-0.076	(from plot)						

Tube #2

Time (min)	RPM:	Acceleration (cm/s^2):	Gravity:	ln (g):	Tube Height:	Height(cm):	Change in	% Change in	Py (kPa)	ϕ	Ps
					18.22	8.22	Tube Height	Tube Height			(%)
0	0.00	981.00	1.00	0.00	13.1	3.1			0.18	0.42	66%
60	300.00	10800.00	11.01	2.40	12.8	2.8	0.3	10%	2.04	0.47	70%
120	400.00	19200.00	19.58	2.97	12.7	2.7	0.1	0.032258065	3.64	0.49	72%
180	600.00	43200.00	44.05	3.79	12.7	2.7	0	0	8.18	0.49	72%
240	800.00	76800.00	78.31	4.36	12.7	2.7	0	0	14.55	0.49	72%
300	1000.00	120000.00	122.37	4.81	12.7	2.7	0	0	22.73	0.49	72%
360	1200.00	172800.00	176.21	5.17	12.7	2.7	0	0	32.73	0.49	72%
										0.33	

Soil:	Tully 105µm-177µm	(#)	**Specific Gravity:**	2.66	(#)						
Percent Solids:	33.00	(%)	**Density water:**	1.00	(gm/cm^3)						
Radius:	12.00	(cm)	**Volume Fraction:**	0.16							
Mass solid:	16.50	(gm)									
Mass water:	33.50	(gm)	**Slope S:**	-0.0943	(from plot)						

Tube #3

Time (min)	RPM:	Acceleration (cm/s^2):	Gravity:	ln (g):	Tube Height:	Height(cm):	Change in	% Change in	Py (kPa)	ϕ	Ps
					78.2	8.2	Tube Height	Tube Height			(%)
0	0.00	981.00	1.00	0.00	73.05	3.05			0.18	0.43	67%
60	300.00	10800.00	11.01	2.40	72.75	2.75	0.3	10%	2.04	0.48	71%
120	400.00	19200.00	19.58	2.97	72.7	2.7	0.05	2%	3.63	0.49	72%
180	600.00	43200.00	44.05	3.79	72.6	2.6	0.1	3%	8.20	0.51	73%
240	800.00	76800.00	78.31	4.36	72.6	2.6	0	0%	14.58	0.51	73%
300	1000.00	120000.00	122.37	4.81	72.6	2.6	0	0%	22.78	0.51	73%
360	1200.00	172800.00	176.21	5.17	72.6	2.6	0	0%	32.81	0.51	73%
										0.35	

Soil:	Tully 105µm-177µm	(#)	**Specific Gravity:**	2.66	(#)						
Percent Solids:	33.00	(%)	**Density water:**	1.00	(gm/cm^3)						
Radius:	12.00	(cm)	**Volume Fraction:**	0.16							
Mass solid:	16.50	(gm)									
Mass water:	33.50	(gm)	**Slope S:**	-0.0847	(from plot)						

Tube #4

Time (min)	RPM:	Acceleration (cm/s^2):	Gravity:	ln (g):	Tube Height:	Height(cm):	Change in	% Change in	Py (kPa)	ϕ	Ps
					98.2	8.2	Tube Height	Tube Height			(%)
0	0.00	981.00	1.00	0.00	93.1	3.1			0.18	0.42	66%
60	300.00	10800.00	11.01	2.40	92.8	2.8	0.3	10%	2.03	0.47	70%
120	400.00	19200.00	19.58	2.97	92.7	2.7	0.1	3%	3.63	0.49	72%
180	600.00	43200.00	44.05	3.79	92.67	2.67	0.03	1%	8.17	0.49	72%
240	800.00	76800.00	78.31	4.36	92.66	2.66	0.01	0%	14.54	0.49	72%
300	1000.00	120000.00	122.37	4.81	92.65	2.65	0.01	0%	22.73	0.50	72%
360	1200.00	172800.00	176.21	5.17	92.65	2.65	0	0%	32.73	0.50	72%
										0.34	

Soil:	Ottawa 250µm-297µm	(#)	**Specific Gravity:**	2.63	(#)						
Percent Solids:	33.00	(%)	**Density water:**	1.00	(gm/cm^3)						
Radius:	12.00	(cm)	**Volume Fraction:**	0.16							
Mass solid:	16.50	(gm)									
Mass water:	33.50	(gm)	**Slope S:**	-0.0223	(from plot)						

Tube #1

Time (min)	RPM:	Acceleration (cm/s^2):	Gravity:	ln (g):	Tube Height: 37.3	Height(cm): 8.3	Change in Tube Height	% Change in Tube Height	Py (kPa)	ϕ	Ps (%)
0	0.00	981.00	1.00	0.00	31.6	2.6			0.19	0.51	73%
60	300.00	10800.00	11.01	2.40	31.5	2.5	0.1	4%	2.06	0.53	75%
120	400.00	19200.00	19.58	2.97	31.48	2.48	0.02	1%	3.67	0.53	75%
180	600.00	43200.00	44.05	3.79	31.48	2.48	0	0%	8.26	0.53	75%
240	800.00	76800.00	78.31	4.36	31.48	2.48	0	0%	14.69	0.53	75%
300	1000.00	120000.00	122.37	4.81	31.48	2.48	0	0%	22.95	0.53	75%
360	1200.00	172800.00	176.21	5.17	31.48	2.48	0	0%	33.05	0.53	75%
										0.38	

Soil:	Ottawa 250µm-297µm	(#)	**Specific Gravity:**	2.63	(#)						
Percent Solids:	33.00	(%)	**Density water:**	1.00	(gm/cm^3)						
Radius:	12.00	(cm)	**Volume Fraction:**	0.16							
Mass solid:	16.50	(gm)									
Mass water:	33.50	(gm)	**Slope S:**	-0.0184	(from plot)						

Tube #2

Time (min)	RPM:	Acceleration (cm/s^2):	Gravity:	ln (g):	Tube Height: 51.35	Height(cm): 8.35	Change in Tube Height	% Change in Tube Height	Py (kPa)	ϕ	Ps (%)
0	0.00	981.00	1.00	0.00	45.6	2.6			0.19	0.51	73%
60	300.00	10800.00	11.01	2.40	45.58	2.58	0.02	1%	2.07	0.52	74%
120	400.00	19200.00	19.58	2.97	45.55	2.55	0.03	0.011538462	3.68	0.52	74%
180	600.00	43200.00	44.05	3.79	45.52	2.52	0.03	0.011538462	8.30	0.53	75%
240	800.00	76800.00	78.31	4.36	45.52	2.52	0	0	14.75	0.53	75%
300	1000.00	120000.00	122.37	4.81	45.52	2.52	0	0	23.04	0.53	75%
360	1200.00	172800.00	176.21	5.17	45.52	2.52	0	0	33.18	0.53	75%
										0.37	

Soil:	Ottawa 250µm-297µm	(#)	**Specific Gravity:**	2.63	(#)						
Percent Solids:	33.00	(%)	**Density water:**	1.00	(gm/cm^3)						
Radius:	12.00	(cm)	**Volume Fraction:**	0.16							
Mass solid:	16.50	(gm)									
Mass water:	33.50	(gm)	**Slope S:**	-0.0376	(from plot)						

Tube #3

Time (min)	RPM:	Acceleration (cm/s^2):	Gravity:	ln (g):	Tube Height: 60.3	Height(cm): 8.3	Change in Tube Height	% Change in Tube Height	Py (kPa)	ϕ	Ps (%)
0	0.00	981.00	1.00	0.00	54.7	2.7			0.19	0.49	72%
60	300.00	10800.00	11.01	2.40	54.6	2.6	0.1	4%	2.05	0.51	73%
120	400.00	19200.00	19.58	2.97	54.55	2.55	0.05	2%	3.66	0.52	74%
180	600.00	43200.00	44.05	3.79	54.52	2.52	0.03	1%	8.25	0.52	74%
240	800.00	76800.00	78.31	4.36	54.52	2.52	0	0%	14.66	0.52	74%
300	1000.00	120000.00	122.37	4.81	54.52	2.52	0	0%	22.91	0.52	74%
360	1200.00	172800.00	176.21	5.17	54.52	2.52	0	0%	32.98	0.52	74%
										0.37	

Soil:	Ottawa 250µm-297µm	(#)	**Specific Gravity:**	2.63	(#)						
Percent Solids:	33.00	(%)	**Density water:**	1.00	(gm/cm^3)						
Radius:	12.00	(cm)	**Volume Fraction:**	0.16							
Mass solid:	16.50	(gm)									
Mass water:	33.50	(gm)	**Slope S:**	-0.0412	(from plot)						

Tube #4

Time (min)	RPM:	Acceleration (cm/s^2):	Gravity:	ln (g):	Tube Height: 48.35	Height(cm): 8.35	Change in Tube Height	% Change in Tube Height	Py (kPa)	ϕ	Ps (%)
0	0.00	981.00	1.00	0.00	42.7	2.7			0.19	0.49	72%
60	300.00	10800.00	11.01	2.40	42.58	2.58	0.12	4%	2.07	0.52	74%
120	400.00	19200.00	19.58	2.97	42.55	2.55	0.03	1%	3.68	0.52	74%
180	600.00	43200.00	44.05	3.79	42.5	2.5	0.05	2%	8.30	0.53	75%
240	800.00	76800.00	78.31	4.36	42.5	2.5	0	0%	14.76	0.53	75%
300	1000.00	120000.00	122.37	4.81	42.5	2.5	0	0%	23.07	0.53	75%
360	1200.00	172800.00	176.21	5.17	42.5	2.5	0	0%	33.21	0.53	75%
										0.37	

Soil:	Ottawa 177µm-250µm	(#)	Specific Gravity:	2.65	(#)
Percent Solids:	33.00	(%)	Density water:	1.00	(gm/cm^3)
Radius:	12.00	(cm)	Volume Fraction:	0.16	
Mass solid:	16.50	(gm)			
Mass water:	33.50	(gm)	Slope S:	-0.0291	(from plot)

Tube #1

Time (min)	RPM:	Acceleration (cm/s^2):	Gravity:	ln (g):	Tube Height: 37.4	Height(cm): 8.4	Change in Tube Height	% Change in Tube Height	Py (kPa)	ϕ	Ps (%)
0	0.00	981.00	1.00	0.00	31.65	2.65			0.19	0.50	73%
60	300.00	10800.00	11.01	2.40	31.55	2.55	0.1	4%	2.10	0.52	74%
120	400.00	19200.00	19.58	2.97	31.5	2.5	0.05	2%	3.74	0.53	75%
180	600.00	43200.00	44.05	3.79	31.5	2.5	0	0%	8.41	0.53	75%
240	800.00	76800.00	78.31	4.36	31.5	2.5	0	0%	14.95	0.53	75%
300	1000.00	120000.00	122.37	4.81	31.5	2.5	0	0%	23.35	0.53	75%
360	1200.00	172800.00	176.21	5.17	31.5	2.5	0	0%	33.63	0.53	75%
										0.38	

Soil:	Ottawa 177µm-250µm	(#)	Specific Gravity:	2.65	(#)
Percent Solids:	33.00	(%)	Density water:	1.00	(gm/cm^3)
Radius:	12.00	(cm)	Volume Fraction:	0.16	
Mass solid:	16.50	(gm)			
Mass water:	33.50	(gm)	Slope S:	-0.0203	(from plot)

Tube #2

Time (min)	RPM:	Acceleration (cm/s^2):	Gravity:	ln (g):	Tube Height: 51.5	Height(cm): 8.5	Change in Tube Height	% Change in Tube Height	Py (kPa)	ϕ	Ps (%)
0	0.00	981.00	1.00	0.00	45.65	2.65			0.19	0.51	73%
60	300.00	10800.00	11.01	2.40	45.6	2.6	0.05	2%	2.12	0.52	74%
120	400.00	19200.00	19.58	2.97	45.55	2.55	0.05	0.018867925	3.77	0.53	75%
180	600.00	43200.00	44.05	3.79	45.55	2.55	0	0	8.49	0.53	75%
240	800.00	76800.00	78.31	4.36	45.55	2.55	0	0	15.09	0.53	75%
300	1000.00	120000.00	122.37	4.81	45.55	2.55	0	0	23.58	0.53	75%
360	1200.00	172800.00	176.21	5.17	45.55	2.55	0	0	33.95	0.53	75%
										0.37	

Soil:	Ottawa 177µm-250µm	(#)	Specific Gravity:	2.65	(#)
Percent Solids:	33.00	(%)	Density water:	1.00	(gm/cm^3)
Radius:	12.00	(cm)	Volume Fraction:	0.16	
Mass solid:	16.50	(gm)			
Mass water:	33.50	(gm)	Slope S:	-0.0291	(from plot)

Tube #3

Time (min)	RPM:	Acceleration (cm/s^2):	Gravity:	ln (g):	Tube Height: 60.4	Height(cm): 8.4	Change in Tube Height	% Change in Tube Height	Py (kPa)	ϕ	Ps (%)
0	0.00	981.00	1.00	0.00	54.7	2.7			0.19	0.49	72%
60	300.00	10800.00	11.01	2.40	54.6	2.6	0.1	4%	2.09	0.51	74%
120	400.00	19200.00	19.58	2.97	54.55	2.55	0.05	2%	3.73	0.52	74%
180	600.00	43200.00	44.05	3.79	54.55	2.55	0	0%	8.39	0.52	74%
240	800.00	76800.00	78.31	4.36	54.55	2.55	0	0%	14.91	0.52	74%
300	1000.00	120000.00	122.37	4.81	54.55	2.55	0	0%	23.30	0.52	74%
360	1200.00	172800.00	176.21	5.17	54.55	2.55	0	0%	33.55	0.52	74%
										0.37	

Soil:	Ottawa 177µm-250µm	(#)	Specific Gravity:	2.65	(#)
Percent Solids:	33.00	(%)	Density water:	1.00	(gm/cm^3)
Radius:	12.00	(cm)	Volume Fraction:	0.16	
Mass solid:	16.50	(gm)			
Mass water:	33.50	(gm)	Slope S:	-0.038	(from plot)

Tube #4

Time (min)	RPM:	Acceleration (cm/s^2):	Gravity:	ln (g):	Tube Height: 48.35	Height(cm): 8.35	Change in Tube Height	% Change in Tube Height	Py (kPa)	ϕ	Ps (%)
0	0.00	981.00	1.00	0.00	42.65	2.65			0.19	0.50	73%
60	300.00	10800.00	11.01	2.40	42.5	2.5	0.15	6%	2.09	0.53	75%
120	400.00	19200.00	19.58	2.97	42.45	2.45	0.05	2%	3.72	0.54	76%
180	600.00	43200.00	44.05	3.79	42.45	2.45	0	0%	8.38	0.54	76%
240	800.00	76800.00	78.31	4.36	42.45	2.45	0	0%	14.89	0.54	76%
300	1000.00	120000.00	122.37	4.81	42.45	2.45	0	0%	23.27	0.54	76%
360	1200.00	172800.00	176.21	5.17	42.45	2.45	0	0%	33.50	0.54	76%
										0.38	

Soil:	Ottawa 105µm-177µm	(#)	**Specific Gravity:**	2.67	(#)						
Percent Solids:	33.00	(%)	**Density water:**	1.00	(gm/cm^3)						
Radius:	12.00	(cm)	**Volume Fraction:**	0.16							
Mass solid:	16.50	(gm)									
Mass water:	33.50	(gm)	**Slope S:**	-0.0444	(from plot)						

Tube #1

Time (min)	RPM:	Acceleration (cm/s^2):	Gravity:	ln (g):	Tube Height: 37.55	Height(cm): 8.55	Change in Tube Height	% Change in Tube Height	Py (kPa)	ϕ	Ps (%)
0	0.00	981.00	1.00	0.00	31.75	2.75			0.19	0.49	72%
60	300.00	10800.00	11.01	2.40	31.5	2.5	0.25	9%	2.15	0.54	76%
120	400.00	19200.00	19.58	2.97	31.5	2.5	0	0%	3.83	0.54	76%
180	600.00	43200.00	44.05	3.79	31.5	2.5	0	0%	8.61	0.54	76%
240	800.00	76800.00	78.31	4.36	31.5	2.5	0	0%	15.31	0.54	76%
300	1000.00	120000.00	122.37	4.81	31.5	2.5	0	0%	23.93	0.54	76%
360	1200.00	172800.00	176.21	5.17	31.5	2.5	0	0%	34.45	0.54	76%
										0.39	

Soil:	Ottawa 105µm-177µm	(#)	**Specific Gravity:**	2.67	(#)						
Percent Solids:	33.00	(%)	**Density water:**	1.00	(gm/cm^3)						
Radius:	12.00	(cm)	**Volume Fraction:**	0.16							
Mass solid:	16.50	(gm)									
Mass water:	33.50	(gm)	**Slope S:**	-0.0479	(from plot)						

Tube #2

Time (min)	RPM:	Acceleration (cm/s^2):	Gravity:	ln (g):	Tube Height: 51.3	Height(cm): 8.3	Change in Tube Height	% Change in Tube Height	Py (kPa)	ϕ	Ps (%)
0	0.00	981.00	1.00	0.00	45.7	2.7			0.19	0.49	72%
60	300.00	10800.00	11.01	2.40	45.5	2.5	0.2	7%	2.09	0.53	75%
120	400.00	19200.00	19.58	2.97	45.48	2.48	0.02	0.007407407	3.72	0.53	75%
180	600.00	43200.00	44.05	3.79	45.45	2.45	0.03	0.011111111	8.38	0.54	76%
240	800.00	76800.00	78.31	4.36	45.45	2.45	0	0	14.90	0.54	76%
300	1000.00	120000.00	122.37	4.81	45.45	2.45	0	0	23.28	0.54	76%
360	1200.00	172800.00	176.21	5.17	45.45	2.45	0	0	33.52	0.54	76%
										0.38	

Soil:	Ottawa 105µm-177µm	(#)	**Specific Gravity:**	2.67	(#)						
Percent Solids:	33.00	(%)	**Density water:**	1.00	(gm/cm^3)						
Radius:	12.00	(cm)	**Volume Fraction:**	0.16							
Mass solid:	16.50	(gm)									
Mass water:	33.50	(gm)	**Slope S:**	-0.0639	(from plot)						

Tube #3

Time (min)	RPM:	Acceleration (cm/s^2):	Gravity:	ln (g):	Tube Height: 60.3	Height(cm): 8.3	Change in Tube Height	% Change in Tube Height	Py (kPa)	ϕ	Ps (%)
0	0.00	981.00	1.00	0.00	54.75	2.75			0.19	0.48	71%
60	300.00	10800.00	11.01	2.40	54.6	2.6	0.15	5%	2.08	0.51	73%
120	400.00	19200.00	19.58	2.97	54.54	2.54	0.06	2%	3.71	0.52	74%
180	600.00	43200.00	44.05	3.79	54.45	2.45	0.09	3%	8.38	0.54	76%
240	800.00	76800.00	78.31	4.36	54.45	2.45	0	0%	14.90	0.54	76%
300	1000.00	120000.00	122.37	4.81	54.45	2.45	0	0%	23.28	0.54	76%
360	1200.00	172800.00	176.21	5.17	54.45	2.45	0	0%	33.52	0.54	76%
										0.38	

Soil:	Ottawa 105µm-177µm	(#)	**Specific Gravity:**	2.67	(#)						
Percent Solids:	33.00	(%)	**Density water:**	1.00	(gm/cm^3)						
Radius:	12.00	(cm)	**Volume Fraction:**	0.16							
Mass solid:	16.50	(gm)									
Mass water:	33.50	(gm)	**Slope S:**	-0.038	(from plot)						

Tube #4

Time (min)	RPM:	Acceleration (cm/s^2):	Gravity:	ln (g):	Tube Height: 48.4	Height(cm): 8.4	Change in Tube Height	% Change in Tube Height	Py (kPa)	ϕ	Ps (%)
0	0.00	981.00	1.00	0.00	42.7	2.7			0.19	0.49	72%
60	300.00	10800.00	11.01	2.40	42.55	2.55	0.15	6%	2.11	0.52	74%
120	400.00	19200.00	19.58	2.97	42.5	2.5	0.05	2%	3.76	0.53	75%
180	600.00	43200.00	44.05	3.79	42.5	2.5	0	0%	8.46	0.53	75%
240	800.00	76800.00	78.31	4.36	42.5	2.5	0	0%	15.04	0.53	75%
300	1000.00	120000.00	122.37	4.81	42.5	2.5	0	0%	23.51	0.53	75%
360	1200.00	172800.00	176.21	5.17	42.5	2.5	0	0%	33.85	0.53	75%
										0.38	